Zhang et al. *NPG Asia Materials* (2020) 12:4
https://doi.org/10.1038/s41427-019-0167-1

NPG Asia Materials

REVIEW ARTICLE Open Access

Pursuit of reversible Zn electrochemistry: a time-honored challenge towards low-cost and green energy storage

Yaojian Zhang[1], Zheng Chen[1], Huayu Qiu[2], Wuhai Yang[3], Zhiming Zhao[1], Jingwen Zhao[1] and Guanglei Cui[1]

Abstract

The world's mounting demands for environmentally benign and efficient resource utilization have spurred investigations into intrinsically green and safe energy storage systems. As one of the most promising types of batteries, the Zn battery family, with a long research history in the human electrochemical power supply, has been revived and reevaluated in recent years. Although Zn anodes still lack mature and reliable solutions to support the satisfactory cyclability required for the current versatile applications, many new concepts with optimized Zn/Zn^{2+} redox processes have inspired new hopes for rechargeable Zn batteries. In this review, we present a critical overview of the latest advances that could have a pivotal role in addressing the bottlenecks (e.g., nonuniform deposition, parasitic side reactions) encountered with Zn anodes, especially at the electrolyte-electrode interface. The focus is on research activities towards electrolyte modulation, artificial interphase engineering, and electrode structure design. Moreover, challenges and perspectives of rechargeable Zn batteries for further development in electrochemical energy storage applications are discussed. The reviewed surface/interface issues also provide lessons for the research of other multivalent battery chemistries with low-efficiency plating and stripping of the metal.

Introduction

With climate warming caused by burning fossil fuels, highly efficient energy storage systems, particularly secondary (i.e., rechargeable) batteries, used for storing intermittent energy from sustainable resources have gained worldwide attention and are bound to increase in demand. Although lithium-ion batteries (LIBs) are currently being considered the most promising technology for transportation-electrification propulsion[1,2], researchers have never stopped exploring alternative and complementary battery chemistries with more distinctive features such as sustainability, safety, and environmental friendliness. Viewed from this perspective, multivalent metal (Zn, Mg, Ca, etc.) batteries (MMBs), based on metallic anodes coupled with cation-intercalation cathodes, are especially attractive because of their resource availability and promising multielectron redox capacity[3,4].

Of the various MMBs, the Zn battery (ZB) family has experienced the longest and richest research history. In 1800, Volta constructed the first battery by stacking alternating Ag and Zn discs separated by a brine-soaked cloth, which produced a steady electric current. In 1836, Daniel introduced the first practical galvanic battery ($Zn/ZnSO_4 + CuSO_4/Cu$), which also employed Zn as the electrode material. The next breakthrough was the invention of the $Zn/NH_4Cl/(MnO_2/C)$ battery by Georges Leclanchè in 1866, which significantly promoted the development of single-use energy-storage devices[5]. Despite the current popularity of LIBs, primary ZBs remain available commercially by virtue of the high cost

Correspondence: Jingwen Zhao (zhaojw@qibebt.ac.cn) or Guanglei Cui (cuigl@qibebt.ac.cn)
[1]Qingdao Industrial Energy Storage Research Institute, Qingdao Institute of Bioenergy and Bioprocess Technology, Chinese Academy of Sciences, Qingdao 266101, China
[2]College of Chemistry and Molecular Engineering, Qingdao University of Science and Technology, Qingdao 266042, China
Full list of author information is available at the end of the article.
These authors contributed equally: Yaojian Zhang, Zheng Chen

performance, innate use/material safety, and mature technology of scale-up production. However, ZBs currently can hardly meet the requirements of cyclic utilization in electronic devices, electric vehicles or large-scale energy storage systems. For an ideal rechargeable ZB, the Zn anode is oxidized to generate Zn^{2+} or $Zn(OH)_4^{2-}$, depending on the type of electrolyte, upon discharge, while a reduction reaction takes place on the cathode side[5]. During recharging, an external electrical potential is applied to deposit Zn and oxidize the cathode, as illustrated in Fig. 1. The cathode materials vary from transition metal-based oxides, Prussian salts, and organic compounds to O_2[6].

While recent years have witnessed a renewed focus in the development of advanced ZB systems designed by various electrode couples and an array of electrolytes, critical issues at the electrolyte-Zn interface remain unsolved. The most commonly used electrolytes for ZBs are routine aqueous solutions, which seem compatible but are detrimental to the Zn metal from both electrochemical and thermodynamic aspects[7]. Aqueous electrolytes, even under neutral or mildly acidic conditions, corrode and passivate Zn, blocking effective Zn^{2+} transport. Moreover, the competitive H_2 evolution at the anode side inevitably disturbs the normal recharging process; the resulting change in local pH increases the accumulation of Zn^{2+}-insulating byproducts on the anode surface. Another main obstacle encountered in the recharging process of Zn anodes lies in the notorious uneven Zn deposition, as represented by dendrite formation and shape change. Zn dendrites often pierce the separator and short-circuit the battery, while the morphology change of Zn anodes induces the formation of "dead" Zn and hence low Coulombic efficiency (CE). Therefore, the realization of "practically" reversible Zn anodes relies on the fulfillment of two requisites: homogenous Zn deposition and side-reaction suppression.

So far, several previous studies have provided excellent reviews on ZBs covering Zn^{2+}-storage electrodes and the corresponding electrolyte systems[4,6,8,9]. Nevertheless, in light of the latest progress, an up-to-date account of the current status and challenges of reversible Zn chemistry has become highly necessary. In this review, we focus on recent progress in achieving homogenous Zn deposition and side-reaction suppression with an emphasis on electrolyte modulation, artificial interphase engineering, and electrode structure design. Furthermore, we present perspectives on the current limitations and attempt to point out future research directions to overcome challenges on the way to utilizing Zn anodes in rechargeable systems.

Novel electrolyte systems

Since the invention of rechargeable ZBs, most studies on Zn plating/stripping or Zn^{2+} ion (de)intercalation in host materials have been performed in routine salt-in-water aqueous electrolytes. To solve the problems of Zn dendrite growth and severe side reactions during cycling, many kinds of additives including polymers, surfactants, and metal ions have been developed. The adsorption of polymers and organic molecules has been demonstrated to increase the polarization for Zn reduction and enable high-quality Zn deposition, while the prior reduction of metal ion additives could serve as the substrate for Zn deposition and suppress Zn dendrites by optimizing the current distribution[10]. Very recently, concentrated aqueous electrolytes have been proposed as promising candidates to suppress hydrogen evolution and expand the electrochemical stability window of aqueous ZBs[11]. However, the utilization of neither additives in electrolytes nor concentrated aqueous electrolytes can completely prevent side reactions in most instances, particularly in alkaline medium. Consequently, a series of nonaqueous electrolyte systems have been developed, including organic electrolytes, ionic liquids, and deep eutectic solvents, since the problems associated with H_2 evolution and other water-induced side reactions can be avoided[12]. On the other hand, the precise influence of the present liquid electrolytes on dendrite suppression remains ambiguous. Meanwhile, with the ever-increasing demand for flexible or stretchable batteries in foldable electronic devices, polymer electrolytes have been introduced and can also address the corrosion and dendrite formation of Zn anodes[6]. In the following section, we summarize and discuss novel electrolyte systems for reversible Zn stripping/deposition.

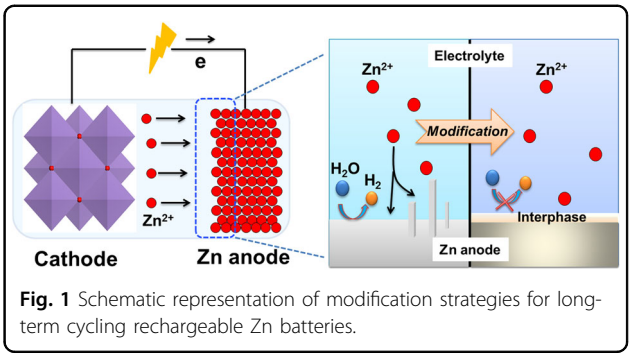

Fig. 1 Schematic representation of modification strategies for long-term cycling rechargeable Zn batteries.

Concentrated aqueous electrolytes

Aqueous Zn redox chemistry has been extensively studied since aqueous electrolytes are safer, less expensive and more facile than nonaqueous counterparts. Moreover, the high ionic conductivity of the aqueous electrolytes is beneficial for high-rate battery operation. However, as mentioned in the previous section, the challenges associated with Zn electrodes in aqueous electrolytes are mainly induced by dendrite growth, corrosion, and other side reactions, resulting in poor rechargeability. Recently,

the superconcentrated "water-in-salt" electrolyte (WiSE) has been demonstrated to be a promising candidate to suppress hydrogen evolution and expand the electrochemical stability window of aqueous electrolytes in LIBs[13]. WiSEs, a subclass of solvent-in-salt electrolyte systems, are defined as those in which the dissolved salt outnumbers water by both volume and mass. Our group first applied the concept of WiSE for reversible Zn redox chemistry in an aqueous $Zn/LiMn_{0.8}Fe_{0.2}PO_4$ battery containing 21 m (the unit m, namely, mol-salt in kg-solvent, means that the solvent weight, instead of the electrolyte volume, is used as the denominator during the calculation of concentration) LiTFSI (TFSI: bis(trifluoromethanesulfonyl)imide) and 0.5 m $ZnSO_4$ as electrolyte[14]. The resultant battery could withstand more than 150 cycles (0.3 C) without obvious capacity fading and enable a high operating voltage exceeding 1.8 V. Subsequently, Wang et al.[11] presented a highly concentrated electrolyte (HCZE) composed of 1 m $Zn(TFSI)_2$ and 20 m LiTFSI to solve the problems of low CE and undesired dendrite growth during Zn plating/stripping. Combining molecular dynamics (MD) simulations with small-angle neutron scattering (SANS) measurements, they deduced that this excellent Zn reversibility stemmed from the unique solvation-sheath structure: Zn^{2+} is surrounded by $TFSI^-$ instead of water, as shown in Fig. 2. A similar work has been reported by Zhang et al.[15], who adopted a 3 M $Zn(CF_3SO_3)_2$ aqueous solution that enabled ~100% Zn plating/stripping efficiency and Zn dendrite-free morphology with long-term stability.

Although the concept of WiSEs is scientifically enlightening for further research, they can hardly be employed in practical ZBs because of their high cost due to expensive organic metal salts such as $Zn(TFSI)_2$ and $Zn(CF_3SO_3)_2$, which lessens the economic benefits anticipated for ZBs. Thus, zinc chloride ($ZnCl_2$), a rather inexpensive compound and one of the most water-soluble inorganic metal salts, has been used for WiSEs[16]. Very recently, Zhang et al.[17] reported that in a 30 m $ZnCl_2$ electrolyte containing a very small amount of free water molecules, a densely plated Zn metal was produced during the plating/stripping process, while in the dilute $ZnCl_2$ aqueous electrolyte, the Zn anode suffered from a fluffy morphology accompanied by pronounced side reactions that led to the formation of $Zn(OH)_2$ and ZnO. Consequently, the 30 m $ZnCl_2$ electrolyte improved the average CE of Zn plating/stripping to 95.4%, compared to 73.2% in 5 m $ZnCl_2$. Similar observations have been obtained by Chen et al.[18], in which a hydrated $ZnCl_2$ molten salt was developed as the electrolyte for dendrite-free Zn plating/stripping. Raman results suggested that all water molecules participated in Zn^{2+} hydration shells. The resultant Zn-air cell adopting this electrolyte delivered a potentially high energy density and good cyclability, with a reversible capacity of 1000 mAh $g_{(catalyst)}^{-1}$ over 100 cycles. It should be noted that since Cl^- can be oxidized at high voltages, the possible formation of Cl_2 gas evolution should be carefully checked. An effective method to alleviate this side reaction is to select cathode materials

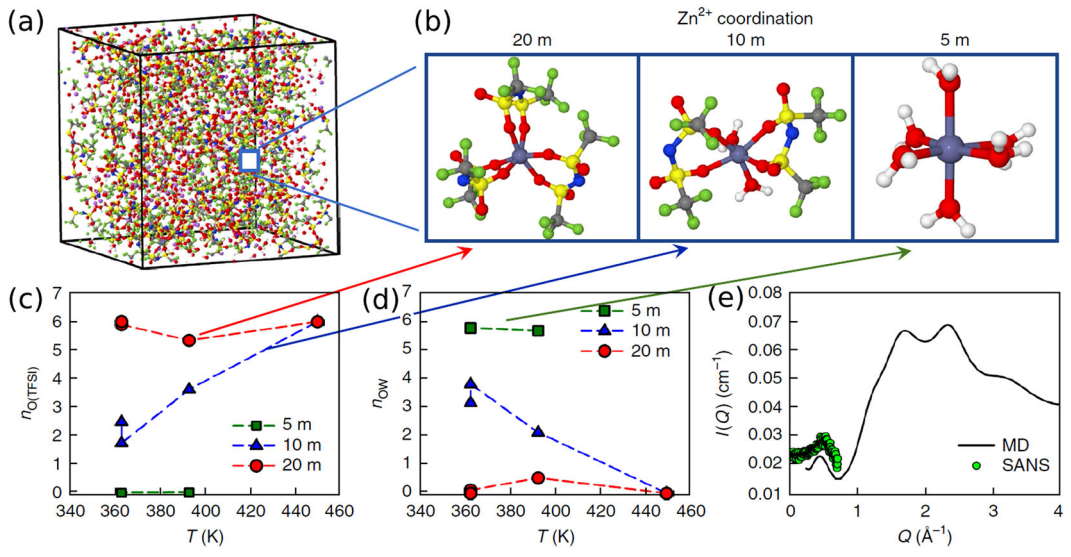

Fig. 2 Molecular dynamics studies of the Zn^{2+}-solvation structure. a Molecular dynamics simulation for HCZE containing 1 m $Zn(TFSI)_2$ and 20 m LiTFSI at 363 K. **b** Illustration of Zn^{2+}-solvation structures in the electrolytes with 1 m $Zn(TFSI)_2$ and varied concentrations of LiTFSI (5 m, 10 m, and 20 m). **c** Zn^{2+}-O(TFSI) and **d** Zn^{2+}-O(water) coordination numbers for HCZE containing 1 m $Zn(TFSI)_2$ and three different concentrations of LiTFSI (5 m, 10 m and 20 m). **e** The small-angle neutron scattering (SANS) curve (green dots) and the simulated results (black line) for HCZE containing 1 m $Zn(TFSI)_2$ and 20 m LiTFSI electrolyte in D_2O (ref. [11]).

with high overpotentials for Cl_2 evolution. The ionic conductivity of concentrated aqueous electrolytes can generally satisfy the demands of most ZBs, and their influence on the rate performance is not significant. However, the salt precipitation and high viscosity from highly concentrated solutions cannot be neglected, especially in the low-temperature range.

Organic electrolytes

Another strategy to alleviate Zn dendrite growth and H_2 evolution relies on utilizing nonaqueous electrolytes consisting of Zn salts and organic solvents. To date, most studies on Zn plating/stripping or Zn^{2+} ion (de)intercalation for rechargeable ZBs have been performed in aqueous electrolytes, while very little information is available in the literature on nonaqueous ZBs[4,19]. Han et al.[12] compared the electrochemical properties of several nonaqueous Zn electrolytes including diglyme-Zn$(TFSI)_2$, acetonitrile-Zn$(CF_3SO_3)_2$, and propylene carbonate-Zn $(TFSI)_2$ electrolytes. They verified that the CE of Zn deposition/dissolution generally exceeded 99% because of the high (electro)chemical stability of metallic Zn in these organic solvents (Fig. 3). Very recently, Naveed et al.[20] reported the adoption of Zn$(CF_3SO_3)_2$ dissolved in triethyl phosphate (TEP) as the electrolyte to achieve a dendrite-free Zn anode with superior cycling stability. Stable Zn plating/stripping with a CE of ~99.7% for over 3000 h can be achieved. In addition, the TEP electrolyte, which is intrinsically nonflammable, could alleviate safety concerns associated with organic solvents. However, organic electrolytes always suffer from relatively large voltage hysteresis and poor rate performance. Combining electrochemical studies, operando XRD and theoretical calculations, Kundu et al.[21] showed that the desolvation penalty of Zn^{2+} ions at the cathode/electrolyte interface is higher in an organic electrolyte composed of Zn $(CF_3SO_3)_2$/acetonitrile than in the aqueous Zn$(CF_3SO_3)_2$ electrolyte, which explains the sluggish interfacial charge transfer in the nonaqueous electrolyte. This work also suggested that the development of nonaqueous Zn ion batteries should focus on methods to reduce the desolvation penalty and inhibit ion pair formation. Given the high charge density of Zn^{2+} ions, polar aprotic solvents, which are commonly used in nonaqueous electrochemistry, such as carbonates and lactones, cannot easily disassociate routine Zn salts. This situation tremendously hinders the number of viable salts that can be used for nonaqueous ZBs.

Ionic liquids and deep eutectic solvents

Ionic liquids (ILs) are another promising alternative to conventional aqueous electrolytes since the problems associated with H_2 evolution and other water-induced side reactions can be avoided. Moreover, ILs are usually nonvolatile and thermostable with no harmful vapors even at high temperature, properties that are preferable for safety concerns[22–24]. Notably, many reports revealed that the Zn/Zn^{2+} redox couple could be supported in ILs and that the anions of ILs play a significant role in defining their properties. Of the many anions that have been investigated (such as PF_6^-, BF_4^-, $TFSI^-$, CF_3SO_3), $TFSI^-$ has attracted the most attention and has been studied by several groups[25–30]. In particular, Steichen et al.[31] reported that highly reversible Zn deposition/stripping behavior was achieved at high current densities of more than 200 mA cm^{-2} in a new IL with a neutral N-alkylimidazole (AlkIm) ligand, denoted as $[Zn(AlkIm)_6][TFSI]_2$. Furthermore, compact and highly crystalline Zn deposits were obtained.

Despite the fact that the TFSI-based ILs have high stability and low viscosity beneficial to ion transport, the economic consideration of using TFS^- has prompted researchers to explore alternative ILs[32]. One class of low-cost and low-viscosity ILs containing the dicyanamide (dca^-) anion has been developed. A recent report by Simons et al.[33] showed that while various Zn salts (Zn $(dca)_2$, Zn$(ac)_2$, Zn$(Cl)_2$, and $ZnSO_4$) were soluble in the IL 1-ethyl-3-methylimidazolium dicyanamide ([EMIM][dca]), the difference of these anions is of vital importance

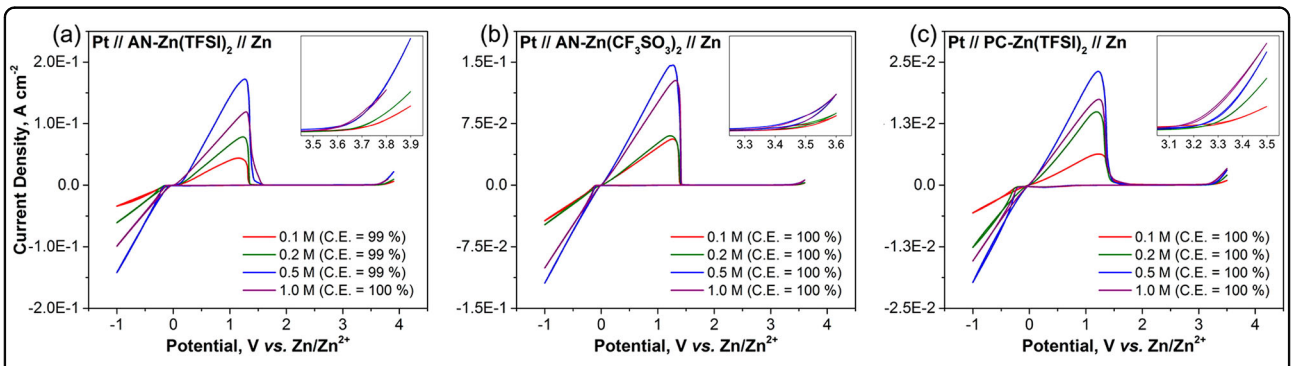

Fig. 3 CV curves of different concentrations of nonaqueous electrolyte. a AN-Zn$(TFSI)_2$, **b** AN-Zn$(CF_3SO_3)_2$, and **c** PC-Zn$(TFSI)_2$. The corresponding CE of Zn deposition/dissolution is also shown. The CV scan rate was 0.1 V s^{-1} (ref. [12]).

for Zn electrodeposition. It was concluded that $Zn(dca)_2$ yielded an 85% Zn plating/stripping CE, and the response current for the Zn redox reaction was 10-fold greater than those found in the studies of Xu[34] and Deng[35], based on $Zn(TFSI)_2$ and $ZnCl_2$, respectively. Since then, the same research group investigated $Zn(dca)_2$ in dca-based ILs both electrochemically and spectroscopically and indicated that the formation of $Zn(dca)_x^{2-x}$ complex anions is responsible for the improved electrochemical properties[32]. The researchers also compared the Zn electrochemistry in imidazolium ([C2mim][dca]) and pyrrolidinium ([C4mpyr][dca]) systems (Fig. 4)[36] and found that the imidazolium system could sustain over 90 deposition/stripping cycles at 0.1 mA cm^{-2}. Xu et al.[34] presented the viewpoint that both cations and anions in ILs exert effects on the Zn redox reactions, while the kinetic behavior of the Zn species is mainly controlled by the type of anions.

ILs are often contaminated with water from manufacturing. In some cases, water is regarded as an impurity that destabilizes the electrochemical window of ILs[37]. However, the addition of water in controlled amounts can reduce the viscosity of the solution, improve the conductivity and thus modify the metal deposition behavior[32,33,35,38–42]. It was confirmed that by introducing 3 wt% H_2O into the IL $[C_4mpyr][dca]$, a higher current density was achieved for the Zn redox reaction along with a more compact and dendrite-free morphology of Zn deposits[43]. In the presence of an alkoxy-ammonium-based IL containing 2.5 wt% H_2O, stable charge/discharge cycling with a reduced activation barrier for Zn deposition can be observed[44]. Recent investigations revealed that the structures and electrochemical properties of the IL-water mixtures are strongly dependent on the interactions between IL components and water[37,45,46]. Specifically, upon the addition of water, the liquid structure gradually changes from that of an IL-like system to that of a typical aqueous solution.

Unfortunately, the current ILs are generally expensive and toxic, which has limited their commercial exploitation[47]. Deep eutectic solvents (DESs) have been recognized as a potential candidate to replace ILs because they are less expensive, biodegradable, and usually promote a high solubility of various metal compounds (such as oxides, sulfides, and chlorides) under mild conditions. Importantly, desirable metal electrodeposits can be obtained in metal ion-containing DESs without any additives[48]. Compared to the study of classical ILs, the research into DESs is comparatively in its infancy, with the first paper on this subject published in 2001[47]. Subsequently, a series of papers have been reported to characterize the physical properties of DESs containing $ZnCl_2$ and diverse H-bond donors such as choline chloride, amides, urea, alcohols, and carboxylic acids[47,49–54]. The

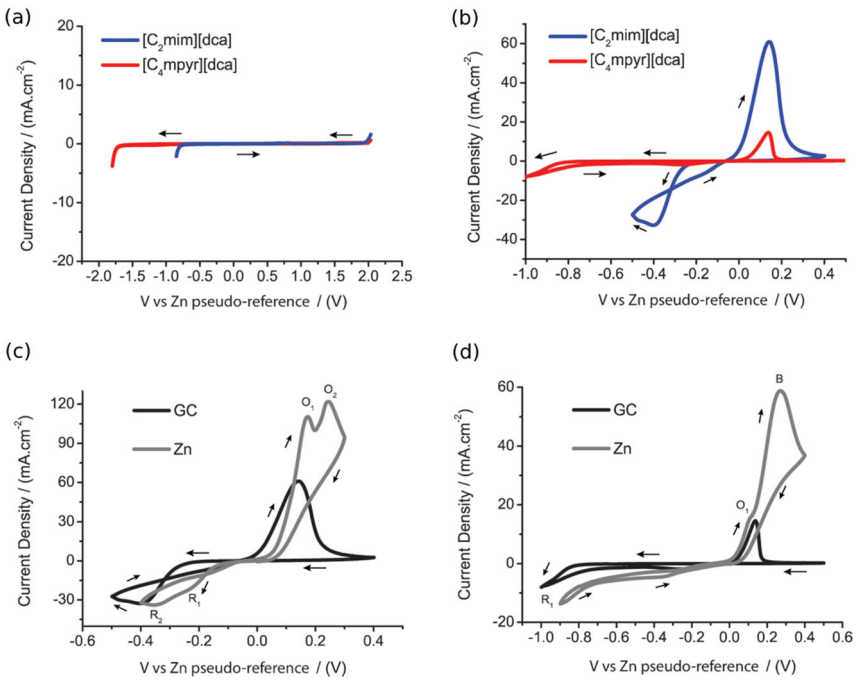

Fig. 4 CV curves of glass carbon electrodes in the presence of different electrolytes. a $[C_2mim][dca]$ and $[C_4mpyr][dca]$ + 3 wt% H_2O. **b** $[C_2mim][dca]$ and $[C_4mpyr][dca]$ + 3 wt% H_2O + 9 mol% $Zn(dca)_2$. **c** $[C_2mim][dca]$ + 3 wt% H_2O + 9 mol% $Zn(dca)_2$. **d** $[C_4mpyr][dca]$ + 3 wt% H_2O + 9 mol% $Zn(dca)_2$. A coiled Zn wire is used as the counter electrode, and the scan rate is 50 mV s^{-1} (ref. [36]).

physical properties of the DESs, as well as the morphology of Zn deposits change, markedly in DESs with different donors. Furthermore, Abbott et al.[55] revealed that nucleation in the urea-based DESs is fast but that bulk growth is slow, whereas a slow nucleation process and relatively fast bulk growth can be obtained in the glycol-based DESs.

Functionally analogous to the ILs, the DES systems also showed decreasing viscosity and increasing conductivity with water as an additive. Recently, Zhao et al.[56] reported a new "water-in-DES" electrolyte, in which all water molecules participated in the DES's internal interaction network, leading to suppressed reactivity with the Zn anode from both thermodynamic and electrochemical aspects (Fig. 5). It is worth underlining that Zn oxide can be dissolved in a choline chloride-based DES, making it possible to use this low-cost Zn source, which can be supplied from the metal refining process and the waste of energy-storage devices[57]. At present, DES electrolytes have been successfully used in secondary ZBs, enabling stable and reversible Zn plating/stripping with enhancement in cycling life compared to that for routine aqueous electrolytes[58–60]. Nevertheless, limited studies on the kinetic properties of Zn species in DESs and their corresponding functionalities on the Zn interface have been reported thus far, which is of particular importance for further cell evaluation and development.

Polymer-based electrolytes

Catering to the ever-increasing demand for flexible and stretchable ZBs, polymer electrolytes have been introduced, the use of which can also serve as an efficient method to address the corrosion and dendrite formation of Zn anodes[6,7,61]. The applied polymers, acting

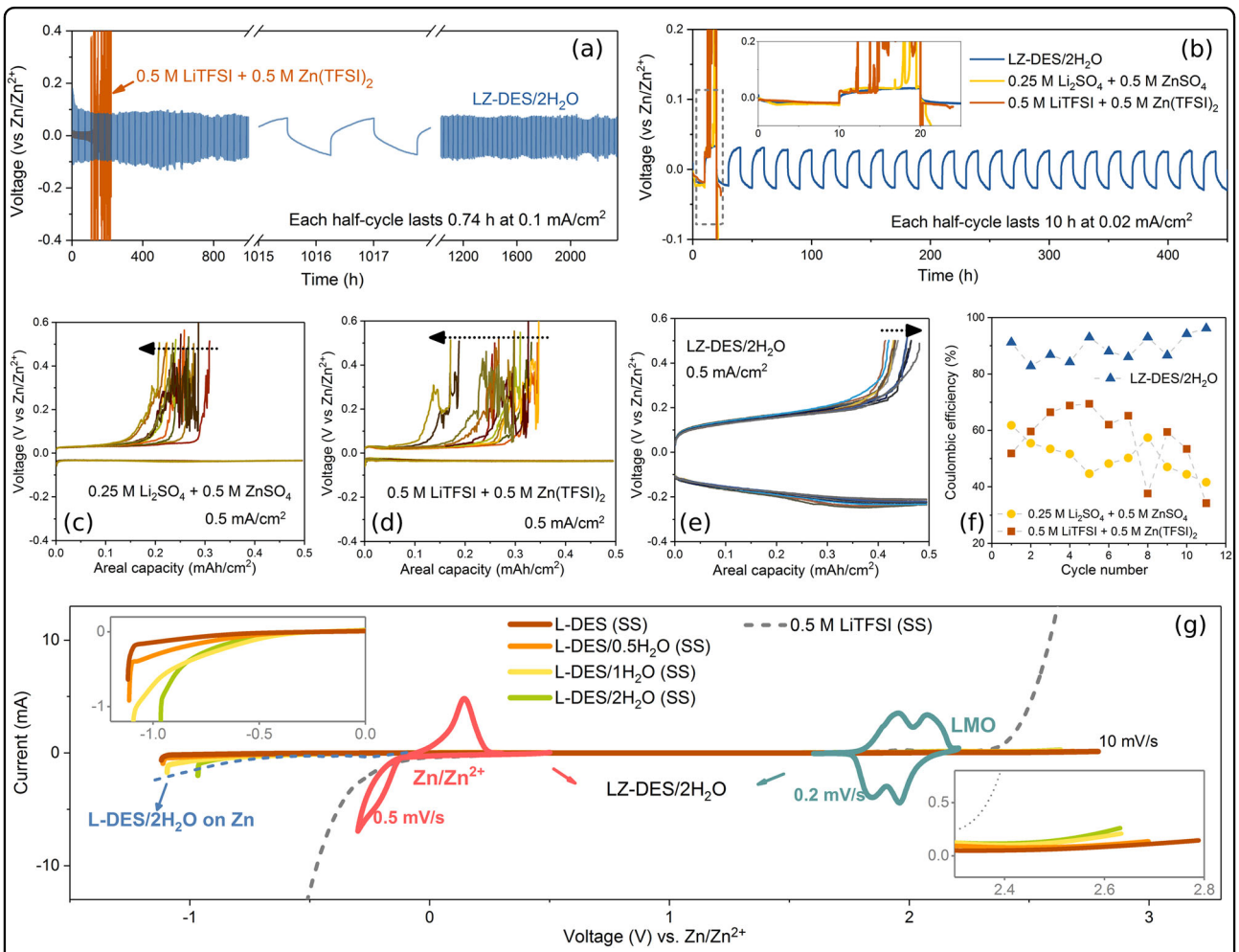

Fig. 5 Electrochemical performances of Zn anodes in different electrolytes. a Typical voltage profiles of Zn/Zn symmetrical cells at a current density of 0.1 mA cm^{-2}. **b** Typical voltage profiles of Zn/Zn symmetrical cells at a current density of 0.02 mA cm^{-2}. **c**–**e** Typical voltage profiles and **f** CE of Zn plating/stripping of Zn/stainless steel (SS) cells in different electrolytes at a current density of 0.5 mAh cm^{-2}. **g** The electrochemical stability window of different electrolytes on the nonactive SS and CV curves of Zn/Zn^{2+} deposition/stripping processes (ref. [56]).

simultaneously as the ion transport media and separator, should encompass certain essential properties[62,63].

(1) High ion conductivity and ion transference number

Due to the complexes formed by the coordination of ions and polymer segments, ion transport has been described as repeated coordination/dissociation of ions among these complexation sites facilitated by molecular chain motions and bond rotations. Thus, a flexible polymer composed of polar segments, such as −O−, −OH, and −C=O should be an optimal choice for high Zn^{2+} conductivity. In analogy with that in rechargeable LIBs, to guarantee that the system discharges at the mA cm^{-2} level, the polymer electrolyte should possess an ion conductivity at a magnitude of 0.1 mS cm^{-1} at room temperature[62]. However, this requirement is quite challenging for the divalent Zn^{2+} ion because its higher charge density than that of Li^+ gives rise to strong interactions with polymers and massive diffusion barriers.

The ion transference number refers to the ratio of charge transported by Zn ionic species to the entire transported charge. Most of the electrolytes show low transference numbers (< 0.5), mainly owing to the simultaneous migration of relevant Zn ions and their counter anions, which could increase the concentration polarization and minimize the cell power density. Anchoring counter particles by dipole-dipole interactions or covalent bonds with designed polymer chains may optimize the ion transference number.

(2) Low glass transition temperature (T_g)

The ion conductivity is claimed to correlate with the polymer segment motion[64]. Thus, a low T_g facilitating the polymer chain mobility is preferable for the enhancement in ion conductivity at ambient temperature.

(3) Mechanical and (electro)chemical stability

In the case of coin cells, where the electrolyte would be sandwiched between stiff shells, mechanical stability does not seem to be an urgent need, but it is indispensable for stretchable electronic devices and scalable industrial manufacture. Although the electrochemical window for ZBs is relatively narrow, (electro)chemically stable electrolytes compatible with electrode materials are essential for the long-term cycling of batteries.

(4) Salt-dissociation capability

Polymers with high polarity are preferred for the incorporation of Zn salts. Instead of the total salt amount in the electrolyte, the amount of dissociated ions directly dictates the ion conductivity and could be increased by polymer matrixes with a high dielectric constant.

Regarding the transport of multivalent ions, polymer-based electrolytes including gel polymer electrolytes (GPEs) and solid polymer electrolytes (SPEs), with and without a liquid plasticizer, respectively, suffer from low ion conductivity and poor rate capability. Thus, diverse polymer electrolyte systems (Scheme 1) for transporting Zn^{2+} have been modified and evaluated, which are highlighted in the following sections.

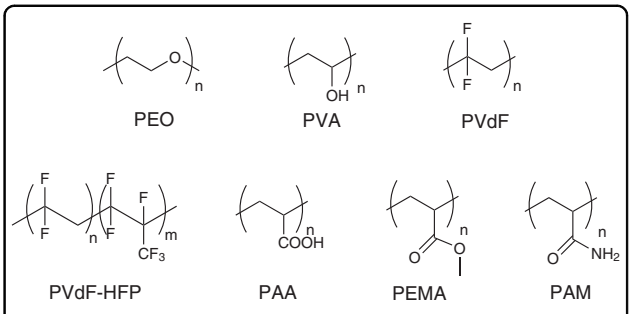

Scheme 1 Polymer structures evaluated for Zn electrolytes.

PEO and its derivatives

Since polyethylene oxide (PEO, Scheme 1) was confirmed to be an ion transporter after mixing with metal salts in the early 1970s[65], PEO and its derivatives have been intensively developed as a vast number of electrolyte systems for a variety of metal ions (such as Li^+, Na^+, and Zn^{2+})[66–68], possibly because of its large dielectric constant, relatively low T_g (~ −64 °C) and flexible polymer chains desirable for self-standing membrane preparation. Patrick et al.[69] discovered the first Zn^{2+}-conducting SPE by mixing $Zn(ClO_4)_2$ with PEO, which unfortunately exhibited extremely low ion conductivities of approximately 10^{-5} mS cm^{-1} at 20 °C, far from adequate for practical applications.

Given that the ion conductivity is especially susceptible to interactions among different ions in the salts and ions of polymer segments, researchers have performed investigations on the existing forms of active Zn^{2+} in polymer electrolytes. Equilibrium diagrams are considered to be a convenient way to disclose the component situation and have been drawn by several groups through thermal analysis methods[70,71]. These diagrams, even when applying the same type of samples containing $ZnCl_2$, give several discrepancies, possibly owing to their different thermal histories and/or humidity-containing ratios; however, a distinct similar intermediate compound was detected in samples with a mole ratio of oxyethylene segment/Zn = 4, labeled as PEO_4: $ZnCl_2$. A detailed description of the complex structure did hinder the exploitation of their properties until the work conducted by Staunton and coworkers[72]. In their study, a lower molecular weight (approximately 500 Da) PEO was applied to form a single crystal of PEO_4: $ZnCl_2$, and then, the model was used as a template for elucidating the equivalent complex structure with higher molecular weight. As shown in Fig. 6, a Zn^{2+} ion is located at the turn along a bending PEO chain coordinated with two

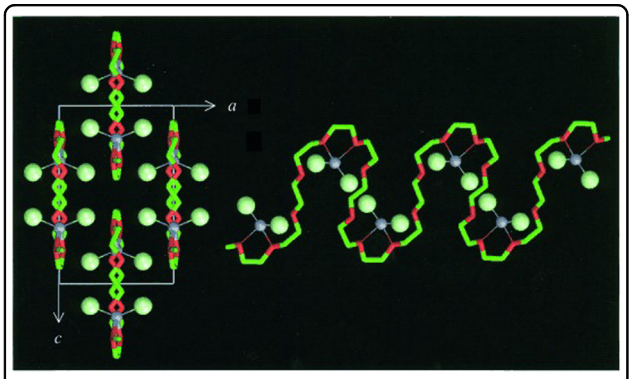

Fig. 6 The single crystal structure of PEO_4: $ZnCl_2$. (Left) The structure of PEO_4: $ZnCl_2$ with four chains in the unit cell. (Right) The coordination of Zn^{2+} within an individual chain. Zn^{2+}: pale gray; chlorine: pale green; carbon: green; oxygen: red (ref. [72]).

neighboring ether oxygen atoms and two Cl^- ions, forming a slightly distorted tetrahedron. Two uncoordinated ether oxygen atoms are retained; four oxygen atoms between each Zn^{2+} ion along the polymer chain accord with the atom mole ratio of PEO_4: $ZnCl_2$.

In addition to $ZnCl_2$, other Zn salts with different counter anions (I^-, Br^-, CH_3COO^-, and $CF_3SO_3^-$)[73–76], playing a crucial role in defining the electrolyte performance, have been thoroughly investigated. Compared to the hot-press casting samples with $Zn(CH_3COO)_2$[75], the SPEs containing $Zn(CF_3SO_3)_2$[76] prepared by a similar process exhibited a higher ion conductivity because of the weaker binding of $CF_3SO_3^-$ to Zn^{2+}. However, the solution casting samples with $Zn(CH_3COO)_2$[74] showed an exceptionally good ion conductivity, surpassing that of Zn $(CF_3SO_3)_2$-containing SPEs, possibly owing to the higher percentage of amorphous phase.

To date, several methods have been implemented to decorate electrolytes with low-grade crystalline polymers. The crystallinity degree of the polymer has a positive correlation with the regularity and symmetry of polymer chains[77]. In the crystal region, polymer chains remain in a systematic pleating form. The introduction of a hetero- or crosslinking segment into the polymer could effectively enable compact parallel packing. To obtain an entirely amorphous electrolyte, sol-gel-derived di-urea crosslinked PEO/siloxane ormolytes were prepared[78]. Although a crystalline PEO/$Zn(CF_3SO_3)_2$ hybrid was observed at an equimolar ratio of the oxyethylene segment to Zn^{2+}, the entirely amorphous complex can be formed as the mole ratio increases to 5, and the maximal conductivity reaches 3×10^{-3} mS cm^{-1} at a mole ratio of 60 under 30 °C. Although the chemical modification method is effective, the processes tend to be complex.

Incorporation of other additives into the polymer system through a physical blending method is an easy and attractive strategy to disturb nucleation and crystal growth. Furthermore, new features could be realized from the additives and the interaction among the mixing materials. Numerous attempts have been made and are summarized as follows.

Nanosized materials have been recognized as promising fillers. Their large specific surface area maximizes contact space with the polymer, retarding the ordered alignment for polymer chains and facilitating ion diffusion[65]. Many researchers have paid much attention to inorganic mineral fillers, such as Al_2O_3[79], TiO_2[80], ZrO_2[81], and SiO_2[82]. It is noticeable that the PEO-PPG-$Zn(CF_3SO_3)_2$ (PPG, polypropylene) SPEs with 3 wt% Al_2O_3 provided the lowest crystallinity, the highest ion conductivity (2.1×10^{-2} mS cm^{-1} at 25 °C, approximately one order higher than that of the filler-free system), and a desirable electrochemical stable window (up to 3.6 V, which is fairly adequate for Zn-based primary and rechargeable batteries)[79]. TiO_2 has been studied in nanocomposite polymeric complexes of PEO γ-irradiated at selected doses and containing $ZnCl_2$[80]. Compared to the film without TiO_2, the nanocomposite SPEs showed 10-fold higher conductivities at room temperature, which is possibly ascribed to the decrease in crystallinity and the formation of new ion transport pathways at the TiO_2-polymer interface. In contrast to the traditional viewpoint that mechanical failure occurs easily for polymer-blended inorganic materials, these nanocomposite films show optimized flexibility owing to their higher amorphous phase ratio.

Organic nanomaterials have been tested to endow SPEs with versatile plastically deformed shapes due to their high flexibility. Branched aramid nanofibers made from Kevlar pulp were applied in PEO-based electrolytes containing Zn $(CF_3SO_3)_2$, resulting in an amorphous state of blended polymer and an enhanced ion conductivity of approximately 2.5×10^{-2} mS cm^{-1} at 25 °C. After 50−100 charge-discharge cycles, 96−100% of the CE could be preserved for Zn/MnO_2 batteries constructed with the electrolyte[83]. Based on this high plasticity of the SPEs, the batteries could be corrugated for a variety of deformations, such as square waves and round waves, to powering unmanned aerial vehicles with an extension of the total flight time (Fig. 7).

GPEs containing solvent plasticizers have attracted tremendous attention due to their liquid-like ion conductivity, solid-state dimensional stability and leak-proof properties. Several liquid plasticizers in PEO-based electrolytes have been studied, including water[84], organic solvents (ethylene carbonate (EC) and propylene carbonate (PC))[85] and IL ([EMIM][TFSI])[86]. GPEs with selected materials may realize not only electrochemical improvement but also certain functional or smart features. Cui and coworkers[84] proposed a new GPE with water as a plasticizer, Pluronic (PEO-poly(propylene oxide)-PEO) as a polymer matrix and Li_2SO_4 and $ZnSO_4$ as dopant salts (Fig. 8). This GPE system exhibits reversible sol-gel

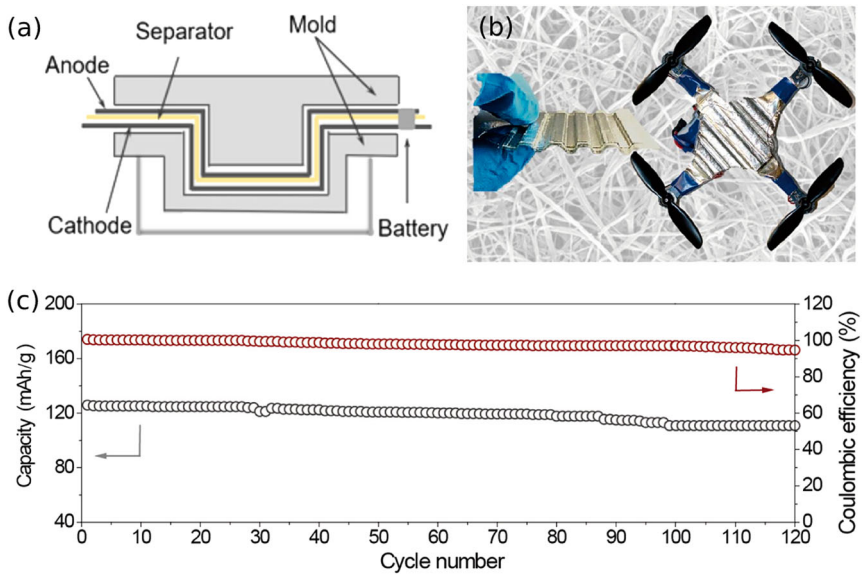

Fig. 7 Preparation and characterization of corrugated Zn/MnO_2 batteries. a Schematic of the mold used for plastic deformation. **b** Drone model with corrugated Zn/MnO_2 batteries. **c** Cycling performance of the Zn/MnO_2 batteries at 0.2 C[83].

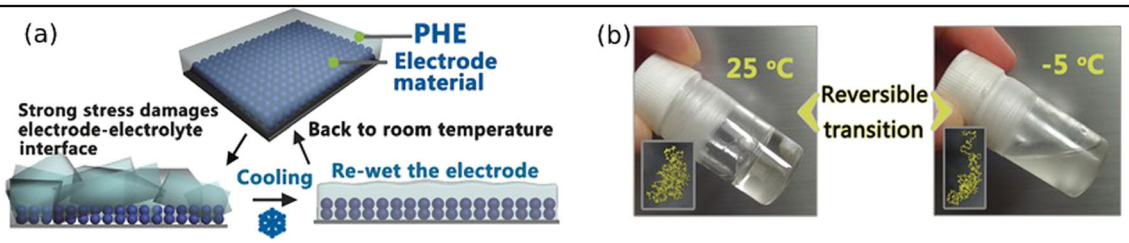

Fig. 8 The reversible sol-gel transition behavior of the PHE system. a The cooling-recovery process with incorporation of the PHE system. **b** Images of PHE and corresponding polymer chain configurations at different temperatures (ref. [84]).

transition behavior under environmental temperature changes: gelation at room temperature and liquidation upon cooling. Hence, in an assembled battery, the cracks at the electrolyte-electrode interface formed by extreme external bending could be completely cured by fusing these separated segments under a simple cooling procedure.

In contrast to the abovementioned batteries with metal ions shuttling back and forth in the electrolyte, alkaline Zn batteries (AZBs) employ hydroxides as complementary migration ions. In general, the operation principle of AZBs is based on a dissolution/precipitation process on the Zn anode side ($Zn + 4OH^- \leftrightarrow Zn(OH)_4^{2-} + 2e^- \leftrightarrow ZnO + 2OH^- + H_2O + 2e^-$) and a hydroxide consumption/generation process on the cathodes composed of O_2, Ni, Co or Mn (taking O_2 as an example: $O_2 + 2H_2O + 4e^- \leftrightarrow 4OH^-$). In addition to the obstacles (i.e., dendrite formation and side reactions) noted in the above sections, there are several other challenges for AZBs: poor stability of polymers under alkaline conditions and diffusion of zincate into electrolytes[6].

Instead of Zn-based salts, KOH has been used intensively as an OH^- source by virtue of its high conductivity, desirable activity, and good low-temperature performance. For the first time, Fauvarque et al.[87] reported the conductivity vs. temperature performance of KOH-containing PEO electrolytes with and without water. The conductivity of the anhydrous sample, reaching 1 mS cm^{-1} at room temperature, was much more pronounced than that of the hydrous sample. Notably, the authors hypothesized that, in addition to the crystalline PEO phase, another phase in hydrous electrolyte systems existed. Thereafter, Guinot et al.[88] performed a thorough investigation of hydrous PEO-based electrolytes containing KOH, which demonstrated the presence of a crystalline complex involving PEO, KOH, and water. A PEO-based copolymer containing epichlorohydrin segments was proposed as an SPE[89].

This electrolyte containing 56 wt% KOH showed a high ion conductivity (typically 1 mS cm^{-1} at room temperature), an anionic transference number of 0.93, and better thermal stability (up to 60 °C) than that of the PEO/KOH/H_2O systems.

PVA and its derivatives

Despite sharing the same constitutional unit formula ($-C_2H_4O-$) with PEO, polyvinyl alcohol (PVA, Scheme 1) contains a pendant $-OH$ for each repeating segment, providing multiple modification possibilities including physical crosslinking via H-bonding, chemical esterification and desirable salt solubility due to its strong polarity. Additionally, a stretchable and electrochemically stable PVA membrane with low T_g is easily prepared due to its uniform and flexible polyolefin main chains. By evaluating PVA-based GPEs with various Zn salts (including $ZnSO_4$, $ZnCl_2$, and $Zn(CF_3SO_3)_2$), Wang et al.[90] found that the ion conductivity based on small-anion salts ($ZnCl_2$ and $ZnSO_4$) was higher than that of large-anion salts ($Zn(CF_3SO_3)_2$).

The PVA-based electrolytes for AZBs have also been studied intensively. Mohamad et al.[91] investigated the effect of the KOH ratio on the properties of PVA-based SPEs. The electrolyte with 40 wt% KOH exhibited the highest room temperature ion conductivity of 0.85 mS m^{-1} and lowest activation energy for the disruption of the crystalline arrangement by alkaline salt. After 100 charge-discharge cycles, the Zn/Ni battery with this electrolyte exhibited 55% capacity retention. $Zn(CH_3COO)_2$ and $Zn(CF_3SO_3)_2$ were tested as a salt mixture in the PVA/KOH system and synergized the thermal stability and ion conductivity of the blended electrolyte[92]. For these two SPEs, that with $Zn(CF_3SO_3)_2$ was found to improve the dimensional stability of PVA/KOH films more distinctly than that with $Zn(CH_3COO)_2$. The highest ion conductivity of 25.5 mS cm^{-1} at room temperature was obtained with an optimum weight ratio of 40/35/25 for PVA/KOH/$Zn(CF_3SO_3)_2$.

For an ideal polymer electrolyte, desirable mechanical and chemical stability should also be taken into account. To fulfill these requirements, poly(epichlorohydrin) (PECH)[93] and PEO/glass fiber[94] were incorporated into PVA/KOH-based SPEs, significantly improving the chemical and mechanical properties. However, a slight decrease in ion conductivity was observed due to the limited KOH weight ratio caused by the hydrophobicity of the incorporated materials.

PVA-based GPEs have been developed mainly for flexible electronics. The impressive electrochemical performance of the hydrogel electrolyte prepared by dissolving PVA into a KOH solution was demonstrated by fiber-shaped Ni-NiO/Zn rechargeable batteries, which achieved an unprecedented cyclic durability (almost no capacity attenuation after 10000 charge-discharge cycles at 22.2 A g^{-1}), outperforming the battery assembled with aqueous electrolytes (96.6% capacity retention after 10000 cycles)[95]. Additives have been applied in PVA/KOH-based GPEs for two main purposes: improving the mechanical properties and stabilizing the electrodes[94,96–99]. In a Zn/Ag battery, cellophane film was embedded in the electrolyte as a separator to mitigate the migration of silver ions into the electrolyte, prolonging the cycle life[99]. The addition of PEO was demonstrated to improve the electrolyte flexibility with a maximal strain of 300%, enhancing the battery elongation to 10%. Correspondingly, the electrolyte with 8.3 wt% KOH shows a high ion conductivity of 300 mS cm^{-1}, similar to that of KOH aqueous with the same concentration[94]. Yang et al.[97] reported that black phosphorous in the GPE could limit $Zn(OH)_4^{2-}$ diffusion, suppress zinc dendrite growth and inhibit Zn corrosion and H_2 evolution reactions. The Zn/Ni battery with this electrolyte exhibited a high initial discharge capacity of 509.8 mAh g^{-1} and retained a value of 212.8 mAh g^{-1} after 100 cycles.

PVdF and its derivatives

Polyvinylidene fluoride (PVdF, Scheme 1) has been developed as the polymer matrix of electrolytes by virtue of its high bond dissociation energy (C-F, 497 kJ mol^{-1}) and dielectric constant ($\varepsilon = 8.4$), endowing electrolytes with desirable chemical stability and salt ionization capability. Despite a low T_g of −40 °C, PVdF, with high crystallinity and a melting point of 171 °C, exhibits good mechanical properties as promising features for practical applications. Rathika and coworkers[86,100] performed a thorough examination of PVdF for SPEs and GPEs containing PEO with various amounts of $Zn(CF_3SO_3)_2$ as the dopant salt. For the SPEs, a reduced crystallinity of the host blend matrix was confirmed, and the highest ionic conductivity reached 2.5×10^{-2} mS cm^{-1} at room temperature in the case of the optimized $Zn(CF_3SO_3)_2$ ratio, beyond which the conductivity reduced to a magnitude of 10^{-3} mS cm^{-1} due to ion reassociation. The ion conductivity of GPEs containing 7 wt% of the IL [EMIM][TFSI] reached 0.163 mS cm^{-1} at room temperature, approximately 10-fold higher than that of SPEs with the same basic components.

As a PVdF derivative, poly(vinylidenefluoride-co-hexafluoropropylene) (PVdF-HFP, Scheme 1) has been widely employed as the polymer host for advanced electrolytes. Its high dielectric constant value and low T_g enable ionization of Zn salts and ion transport in conjunction with polymer chain motion. Johnsi et al.[81,101,102] reported nanocomposite SPEs based on PVdF-HFP and Zn$(CF_3SO_3)_2$ containing different inorganic fillers (i.e., TiO_2, ZrO_2, and CeO_2). Three composite materials showed similar features: the maximum ion conductivity and

amorphous ratio could be achieved for the samples with ~5 wt% nanomaterials (5 wt% for TiO_2 and CeO_2, 7 wt% for ZrO_2). It was also found that the SPEs with ZrO_2 exhibited the best ion conductivity performance (0.46 mS cm^{-1} at 25 °C).

To fabricate GPEs with excellent Zn^{2+}-conducting properties, extensive studies on PVdF-HFP assisted by ILs and organic carbonates as plasticizers have been performed. Xu et al.[85] reported the influence of organic plasticizers (PC and EC), poly(ethylene glycol) dimethyl ethers (PEGDMEs) and Zn salts ($Zn(CF_3SO_3)_2$ and $Zn(TFSI)_2$) on the performance of prepared electrolytes. Incorporation of EC, PEGDME and $Zn(TFSI)_2$ produced large beneficial effects in terms of ion conductivity, reaching 0.47 mS cm^{-1} at 25 °C, as well as other electrochemical properties. However, TGA tests revealed a large weight loss and rapid loss of ion conductivity for the sample containing the EC/PC plasticizer in an open environment.

Romero et al.[103] presented a detailed study on three GPEs based on ILs with the same anion $TFSI^-$ and different cations (1-ethylpyridinium (EPy^+), $EMIM^+$ and trihexyltetradecylphosphonium (P^+) (Scheme 2)). The [P][TFSI] electrolyte was proved to be more resistive than the other electrolytes, which was attributed to the volume barrier of P^+. However, a negligible difference in ion conductivity could be detected for the GPEs containing ILs with the same cation ($EMIM^+$) and different anions (1.31 mS cm^{-1} for $CF_3SO_3^-$ and 1.05 mS cm^{-1} for $TFSI^-$ at 25 °C). In light of the above facts, the electrochemical performance of GPEs is more susceptible to the IL cations than to the IL anions. With the incorporation of ILs, the electrolytes could exhibited exceptional thermal stability with no weight change upon heating to 200 °C. The ZnO nanosized filler in EC/PC/$Zn(CF_3SO_3)_2$/PVdF-HFP systems could increase the Zn^{2+} transference number significantly from 0.35 to 0.55 and preserve the ion conductivity at the same magnitude (~6 mS cm^{-1})[104]. N-Methyl-2-pyrrolidone (NMP) was demonstrated to be a key factor in the $Zn(CF_3SO_3)_2$ and imidazolium-based IL GPE system for improving ion transport owing to the strong interaction between Zn^{2+} and the carbonyl groups of NMP[105,106].

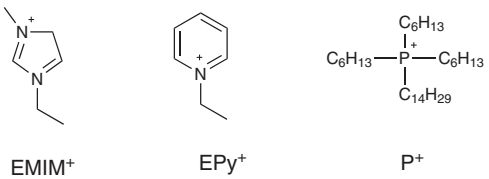

Scheme 2 Chemical structures of the cations ($EMIM^+$, EPy^+ and P^+) (ref. [103]).

Polyacrylic acid and its derivatives

Even though abundant oxygen atoms exist in polyacrylic acid (PAA, Scheme 1), as electron donors play a vital role in Zn salt dissolution and Zn^{2+} coordination, the strong ionic bonds between carboxylate and Zn^{2+} severely obstruct ion transport. In this context, the PAA polymer has been extensively investigated in alkaline conditions for its multiple superior advantages:[107] (1) facilitating OH^- ion transport effectively for flexible molecular chains and anchoring positive ions by carboxylate groups; (2) retaining water up to several hundred times its own weight; (3) surviving in a strong alkaline environment owing to its good chemical stability; (4) maintaining stable mechanical properties under saturated conditions; (5) possessing an easily modified molecular structure for certain property requirements. Note that PAA has been mostly used as the polymer matrix of GPEs, instead of SPEs, due to its relatively high T_g (~103 °C), and a neutralization process has to be applied to eliminate the active proton corrosion detrimental to the Zn anode.

A series of PVA/PAA composite electrolytes incorporated with KOH were investigated, and the highest ion conductivity reached 301 mS cm^{-1} at room temperature, with a weight ratio of PVA/PAA = 10/7.5[108]. Chaduang et al.[109] reported that 3.5 wt% crosslinked PAA in GPEs could obviously change the anode/electrolyte interface structure, preventing the nucleation and growth of Zn dendrites and reducing the interface resistance. A PAA electrolyte neutralized by NaOH could support more than 50 times its own weight of salt solution (0.2 M $Zn(CH_3COO)_2$ and 6 M KOH) at equilibrium and has been used in a variety of batteries[110–112]. The Zn/NiCo hydroxide (indicated as NiCo) batteries assembled with this electrolyte delivered a high initial capacity of 110 mAh g^{-1} and ultralong cycling stability: 10,000 and 16,000 cycles with 73 and 65% capacity retention, respectively, at a high rate of 96 C (Fig. 9)[110]. This kind of electrolyte is also favorable for designing flexible ZBs. An intrinsically 400% stretchable and 50% compressible Zn/NiCo battery was fabricated, which could deliver 87 and 97% of its initial capacity after undergoing a stretching process of 500 cycles and compressing process of 1500 cycles, respectively[111]. Two super-stretchable Zn-air batteries, including a flat-shaped (800% stretchable) and fiber-shaped (500% stretchable) battery, were developed by designing a dual-network electrolyte based on crosslinked PANa incorporated with cellulose[112]. These devices showed stable power output performance even after being heavily deformed, benefiting from the mechanically flexible and alkaline-tolerant properties endowed by the hydrogel electrolyte.

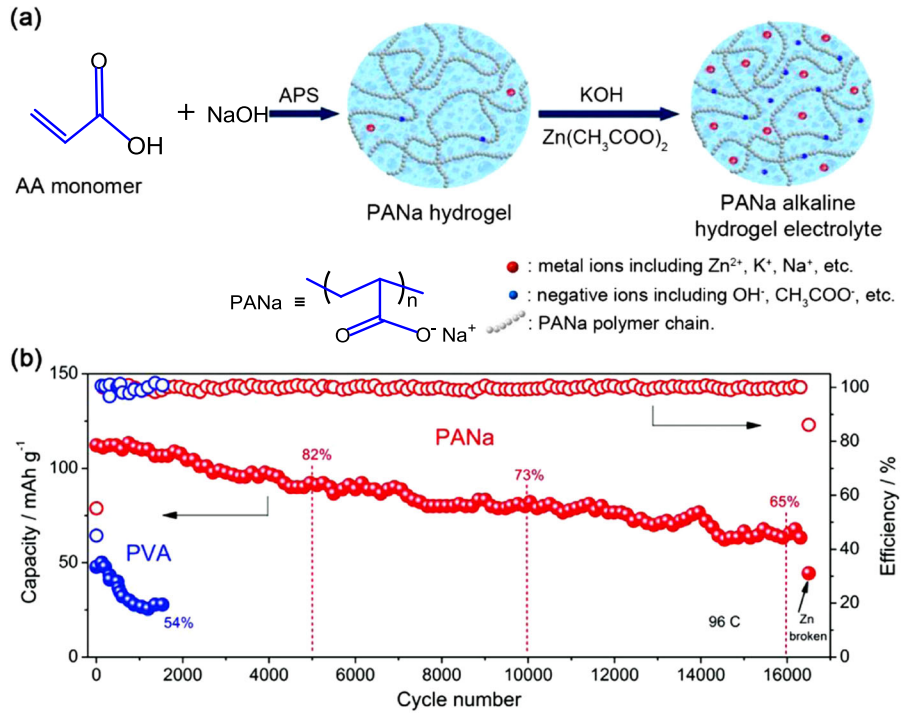

Fig. 9 Synthesis of the PANa electrolyte and the batteries performance. a Preparation of the PANa electrolyte. **b** Long-term cycling performance and the corresponding CE at 96 C rate (ref. [110]).

The esterification of PAA triggers the coordination disruption between Zn^{2+} and carboxylate radicals, paving a new route for their application in Zn^{2+} transporting electrolytes. Suthanthiraraj and coworkers[82,113,114] thoroughly investigated polymer electrolytes based on poly (vinyl chloride) (PVC) and poly(ethyl methacrylate) (PEMA, Scheme 1) containing $Zn(CF_3SO_3)_2$ as the dopant salt. First, the optimized weight ratio of the Zn salt was determined to be 30 wt% according to the thermal stability and electrochemical performance[114]. Then, the authors evaluated the influence of [EMIM][TFSI] on this system and found that the weight ratio of [EMIM][TFSI] in the electrolyte was positively correlated with the dielectric constant, amorphous phase ratio and ion conductivity. The highest ion conductivity could reach 0.11 mS cm^{-1} at room temperature[113,114]. Furthermore, the addition of nanosized SiO_2 in the electrolyte with an optimized composition effectively reduced T_g and increased the thermal stability, electrochemical stability window (5.07 V) and ion conductivity (0.67 mS cm^{-1}) at room temperature[82].

The PAA derivatives via amidation have also been explored as matrixes for GPEs in AZBs[115,116]. Cross-linked polyacrylamide (PAM, Scheme 1) saturated with 6 M KOH solution combined good flexibility and high ion conductivity (330 mS cm^{-1})[115], ensuring no noticeable degradation in power density performance (39 mW cm^{-2}) of Zn-air batteries at a bending angle down to 60°.

Single-ion conductor

Instead of entrapping salt in the polymer matrix through a physical mixing process, some functional groups are anchored on polymer backbones by covalent bonds, namely, single-ion conductors, providing mobile ions by virtue of self-ion-dissociation. Therefore, the ion conductivity only depended on the transport of positive or negative particles owing to their immobilized counterparts, giving rise to an increased ion transference number, battery cycling efficiency and decreased polarization. Polyolefins, as the main chains of single-ion conductors, have been employed intensively for their recognized desirable segment mobility, good mechanical properties, and chemical stability. According to the functional group properties, single-ion conductors are separated into single-anion conductors (SACs) and single-cation conductors (SCCs).

SACs are normally composed of quaternized polymers, are selective to the passage of anions, and are anticipated to pave a new way that preserves positive Zn^{2+} carriers in anodic compartments (Fig. 10). Lin et al.[117] reported that PVA functionalized with quaternary ammonium was used as an electrolyte, which depressed the self-discharge rate of AZB to less than 7% per month due to the inhibition of

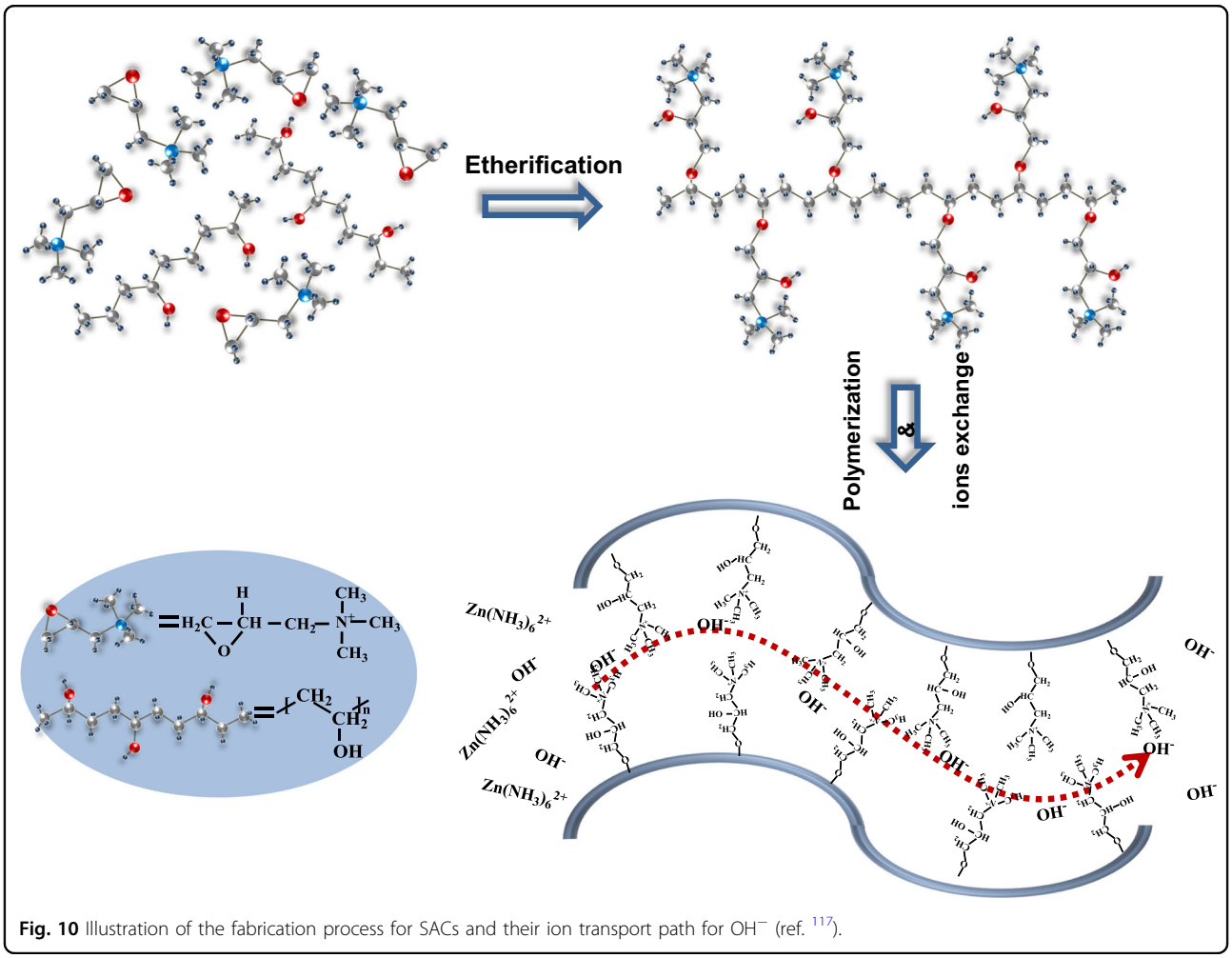

Fig. 10 Illustration of the fabrication process for SACs and their ion transport path for OH^- (ref. [117]).

$[Zn(NH_3)_6]^{2+}$ crossover. To compensate for the limited ion conductivity of nonporous single-ion conductors, a sandwich-type electrolyte configuration was designed. In AZBs, porous separators with an alkaline solution are applied as the center of the electrolyte for high ion conductivity. Thin SAC layers were applied to coat the porous separators and enable OH^- migration while blocking $Zn(OH)_4^{2-}$. Compared to the microporous polyolefin films, the prepared electrolyte gave a 96% decrease in $Zn(OH)_4^{2-}$ crossover and an approximately 3-fold durability improvement in the battery charge/discharge setup[118]. As key components of alkaline exchange membrane fuel cells, SACs have been observed to be vulnerable to degradation in strong alkaline environments. Wei et al.[119] prepared a low-cost SAC (CS-PDDA-OH^-) that exhibits a high OH^- conductivity (24 mS cm^{-1}) with good alkaline stability (preserving a stable ion conductivity performance for 216 h in 8 M KOH at 80 °C) and enables a high power density (48.9 mW cm^{-2}) for Zn-air batteries.

In contrast to SACs, SCCs are functionalized with negatively charged groups (e.g., $-SO_3^-$ and $-COO^-$ as cation coordination points) on main polymer chains. While the SCC should be an effective Zn^{2+} transporter, it is not without obstacles. Zn^{2+} tends to bind to two or more of these negatively charged groups and form weak ion crosslinks that could hamper ion migration, stiffen the material, and alter its solubility. Therefore, limited attempts have been made to certify the validity of SCCs in ZBs. Lee and coworkers[120] synthesized a crosslinked sulfonated polyacrylonitrile (PAN-S), which exhibited an ion conductivity of 8.12×10^{-2} mS cm^{-1} at room temperature without additional salt dopant. In contrast to traditional electrolyte systems with nonwoven separators (Fig. 11), the nonporous PAN-S electrolyte serving as both the polymer electrolyte and the separator could facilitate Zn dendrite suppression, low polarization (< 40 mV) and long cycling performance up to 350 cycles owing to the even ion flux distribution and single cation transport.

Electrolyte additives

The electrolyte additives for enhancing Zn stripping/deposition can be generally classified into three types,

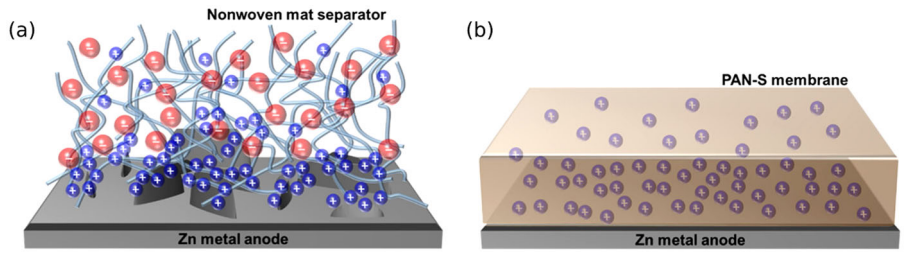

Fig. 11 Schematic descriptions of Zn deposition. a Zn dendrite growth due to the ramified ion deposition on the surface of Zn metal with the conventional separator, **b** dendrite suppression due to the uniform ion deposition with SCC membranes (ref. [120]).

namely, polymers, surfactants, and foreign metal ions. Some organics, such as polymers and surfactants can adsorb on the Zn surface and regulate the local current distribution near the electrode tip, which increases the polarization for Zn reduction[10,121] and thus enables even and smooth Zn deposition[122,123]. Banik et al.[121] reported that polyethylene glycol (PEG), serving as an additive in a halide-based aqueous electrolyte, could effectively suppress dendrite formation during Zn deposition. By using in situ optical microscopy, the effect on dendrite suppression was demonstrated to significantly depend on the PEG concentration (Fig. 12): the higher the PEG concentration was, the lower the exchange current density and thus the higher the suppression efficiency.

Apart from suppressing Zn dendrite formation, many polymers or surfactants can also inhibit competitive side reactions. Hou et al.[124] observed that the addition of sodium dodecyl sulfate (SDS) into the electrolyte could effectively suppress the release of H_2 on the surface of the Zn electrode and extend the cycling lifetime of an aqueous Na/Zn hybrid battery (Fig. 13). Wetting angle measurements and theoretical calculations indicated that SDS adsorbed on the Zn surface via electrostatic adsorption and formed a hydrophobic layer, which prevented direct contact between the electrode and water. Lee et al.[125] demonstrated that the H_2 evolution overpotential was increased enormously and that dendrite formation was suppressed to some extent in the presence of organic acid additives (including TA, SA, PA, and CA, shown in Table 1) with different numbers of polar groups. The authors also suggested that organic surfactants rich in polar groups are helpful in resisting dendrite formation, while those with a small number of polar groups are more effective in alleviating H_2 evolution.

In addition to organics, metal ions (such as Bi^{3+} and Pd^{2+}) with potentials more positive than that of Zn^{2+} can be used as electrolyte additives to regulate Zn deposition[126,127]. These metal ions can be electrodeposited prior to Zn^{2+} reduction; the resulting layer could serve as the substrate for modifying further Zn deposition, which is called the "substrate effect" or "matrix effect"[128,129].

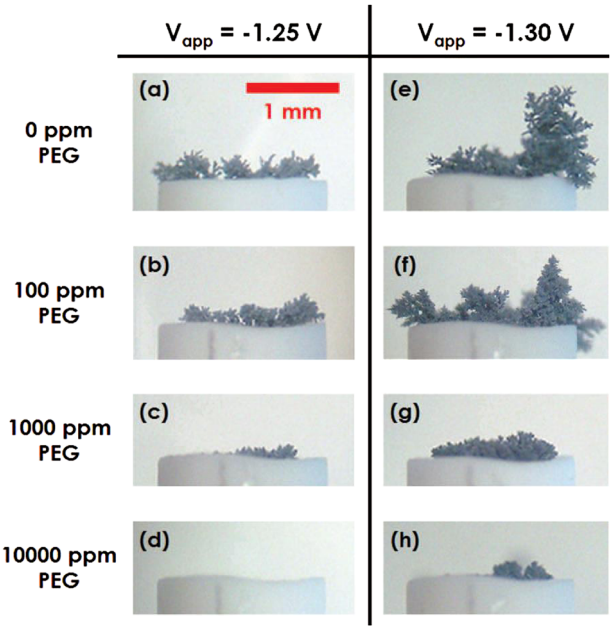

Fig. 12 The evolution of Zn dendrite growth from the tip of a PVC-coated wire electrode observed by optical microscopy. Zn is electrodeposited potentiostatically for approximately 8 min. The electrolyte contains 0.1 M $ZnCl_2$ with a wide range of PEG concentrations as additives (ref. [121]).

Mansfeld et al.[126] found that owing to the presence of Pb^{2+} in an alkaline solution, the Zn deposit tended to be cylindrical and microcrystalline, rather than dendritic. Gallaway et al.[130] investigated the influence of the concentration of a Bi^{3+} additive on the performance of Zn electrodeposition using in situ synchrotron X-rays. Their study showed that a Bi^{3+} additive concentration of 3 ppm resulted in a planar and compact Zn layer when deposited in a flow channel, while a Bi^{3+} concentration above 13 ppm would produce highly irregular layers due to Bi buildup, eventually leading to cell shorting (Fig. 14). Their work highlighted the importance of adequately controlling the concentration of metal ion additives during Zn electrodeposition. In addition, a combination of different

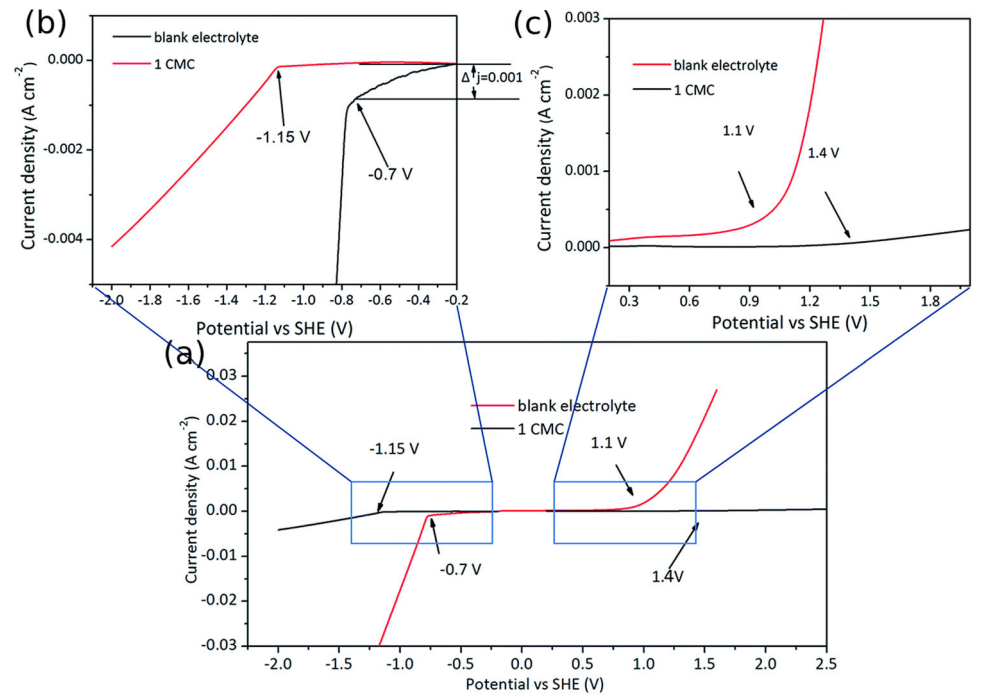

Fig. 13 The influence of SDS additive on the electrochemical window of 1 M $ZnSO_4$ electrolyte. Electrochemical stability window of aqueous electrolytes containing SDS additive obtained from linear sweep voltammetry on titanium grid electrodes versus Ag/AgCl at a scan rate of 10 mV s^{-1} (CMC: critical micelle concentration of the SDS additive) (ref. [124]).

Table 1 Different kinds of additives in the electrolyte to improve the performance of Zn electrode.

Types of additives	Examples	Working mechanism	Ref.
Polymer	Polyethylene glycol (PEG), polyaniline (PANI), PMMA, polyethyleneimine (PEI), polyvinyl alcohol (PVA), polypyrrole, triton X-100	Adsorb on the surface of Zn electrode and slow down the deposition rate of Zn; increase the overpotential of H_2 evolution	121,154–157
Surfactant	Sodium dodecyl sulfate (SDS), thiourea (TU), cetyltrimethylammonium bromide (CTAB), tetrabutylammonium bromide (TBAB), ethylenediamine, succinic acid (SA), tartaric acid (TA), citric acid (CA), vanillin	Adsorb on the surface of Zn electrode to slow down the deposition rate of Zn; increase the overpotential of H_2 evolution	124,125,158–161
Metal cation	Bi^{3+}, Pb^{2+}, In^{3+}	Reduced metal serves as the substrate of Zn deposition and optimize the current distribution of Zn electrode; increase the overpotential of H_2 evolution	126,127,130,162,163

types of additives can be explored to achieve even better cycling performance of Zn electrodes. Wang et al.[127] reported that although the surfactant tetrabutylammonium bromide (TBAB) alone produced a limited effect on dendrite inhibition at high cathodic overpotentials, the joint addition of TBAB and Bi^{3+} resulted in much larger cathodic polarization, effectively suppressing Zn dendrite growth. Relevant types of electrolyte additives are listed in Table 1.

The purpose of using organic additives in the electrolyte is to block the formation sites of dendrites or to decrease the depositing current density to realize more even Zn deposition. However, this would inevitably increase the polarization of the Zn electrode, which could lead to reduced energy conversion efficiency in Zn batteries. Therefore, the amount of organic additives should be appropriate and carefully controlled. In addition, this simple method cannot fundamentally solve the poor

rechargeability of Zn anodes, particularly in an alkaline aqueous medium. For the use of metal ions with a high reduction potential as additives in the electrolyte, more attention should be paid to their possible role in affecting the electrochemical reactions that occur at the cathode side, especially for Zn-based flow batteries[10]. When the metal ions as additives participate in the redox reactions on the cathode side, they interfere with the energy conversion efficiency and cycling performance of the battery. Thus, polymers and organic molecules that mainly involve surface adsorption are more promising as electrolyte additives in ZBs (Table 2)[6,10,12,13,18,21,23,34,51,54,64,68].

Artificial functional interphases

In view of the innately safe, green and low-cost advantages, the century-old ZBs applying aqueous electrolytes are still appealing for future applications in large-scale energy storage and wearable devices. From this context, simultaneously overcoming the bottlenecks of dendrite formation and rampant side reactions while preserving the high aqueous ion conductivity is bound to be challenging, which has stimulated researchers to seek artificial functional interphases for protecting Zn[131]. This interphase could depress corrosion and/or retain valid ion species in the anodic compartment by limiting the direct contact between the electrolyte and the Zn anode. Additionally, the dendrites could be limited by confining the aggregated deposition of Zn^{2+} ions. Moreover, the corresponding negative influence on ion transport can be minimized by controlling the thickness of the coating layer. The necessary properties of materials chosen as artificial functional interphases can be summarized as follows: (1) chemical and electrochemical inertness to electrolyte and anode; (2) tunable ionic permeability and negligible electronic conductivity to harmonize Zn^{2+} migration and Zn nucleation; (3) good anode adhesion capability to buffer the volume change during cycling; and (4) mechanical toughness to maintain the interphase layer geometric stability and depress dendrite growth during electrochemical cycling.

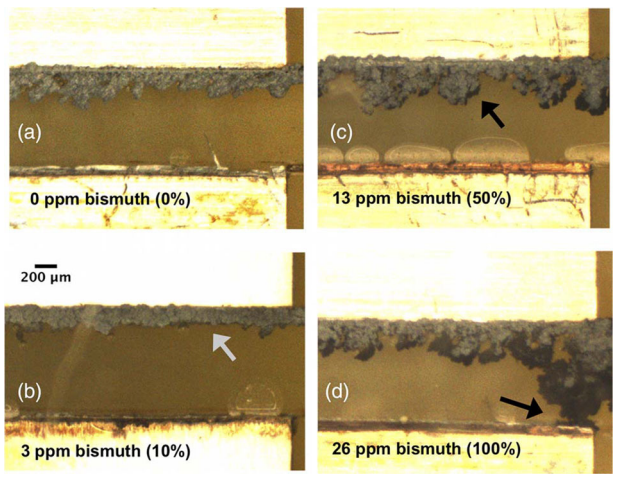

Fig. 14 Optical microscopy of metal layers generated by repeated cycling at a current density of 35 mA cm^{-2} in a flow cell with electrolyte flowing. The top electrode was the working electrode, and the bottom electrode was the counter electrode. Gray arrow: planarized metal layer. Black arrow: macroscopic buildup of bismuth metal (ref. [130]).

Polymer coatings

Compared to inorganic species, polymers as interphase materials have numerous intrinsic merits, including desirable flexibility, easy processability, and controllable modification. Fundamental insights have been conducted to determine the relevant polymer structures. Cui and coworkers[132] proposed a polyamide coating for regulating aqueous Zn electrochemistry and demonstrated that the modified Zn anode exhibited highly reversible dendrite-free plating/stripping with a 60-fold enhancement in cycling performance compared to that of the bare Zn anode. Jo and coworkers[133] found that polyaniline-coated Zn could exhibit 85% corrosion inhibition efficiency

Table 2 Comparison of novel electrolyte systems for reversible Zn stripping/deposition.

Electrolyte systems	Advantages	Disadvantages	Ref.
Concentrated aqueous electrolytes	High ionic conductivity, high safety	High cost in the case of organic zinc salts, water-induced side reactions	13,18
Aqueous electrolyte with additives	High ionic conductivity, low cost, high safety	Water-induced side reactions	6,10
Organic electrolytes	No side reactions	Flammability, large voltage hysteresis	12,21
Ionic liquids	No side reactions, good stability, high safety	High cost, high viscosity, low ionic conductivity	23,34
Deep eutectic solvents	Low cost, biodegradability	High viscosity, low ionic conductivity	51,54
Polymer-based electrolytes	No side reactions, flexibility leak-proof property	Low ionic conductivity, poor interfacial ion transport	64,68

relative to that of pure Zn and enable 97.81% capacity retention after 24 h storage in Zn-air batteries.

PVA, a linear polyhydroxy polymer, has also been chosen as the coating material for protecting Zn anodes due to its film-forming capacity, hydrophilicity and easy chemical modification[134–137]. Zhang et al.[134] reported a PVA layer crosslinked with a glutaraldehyde coater for enhancing the mechanical and chemical stability of Zn anodes. The prepared Zn-air battery exhibited a good capacity retention of up to 90% after 150 cycles, superior to that of the pristine battery. Mechanical and chemical improvements by crosslinking come at the expense of a decrease in ion conductivity due to the confined ion motion space. Thus, SACs have been introduced to provide ionic transport channels in crosslinking coating systems, lowering the polarization of the Zn/Zn^{2+} redox reaction and interfacial resistance[136]. Stock et al.[138] evaluated different coated-Zn electrodes based on commercially available SAC ionomers. As elucidated by electrochemical methods and X-ray photoelectron spectroscopy, a ZnO layer formed between the ionomer coating and Zn electrode, implying that the hydroxide ions could permeate through the coating layer, whereas the oxidized Zn species (i.e., $Zn(OH)_4^{2-}$) was preserved (Fig. 15). In comparison to the bare Zn, the coated Zn achieved up to a 6-fold longer cycle life during the Zn dissolution/deposition process.

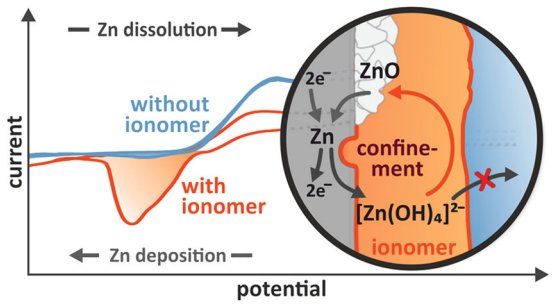

Fig. 15 The discharge and charge process of the Zn anode with and without ionomer in an alkaline electrolyte (ref. [138]).

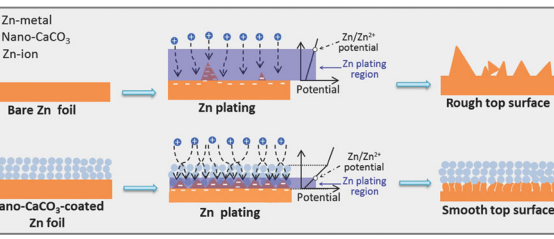

Fig. 16 Schematic illustrations of stabilizing zinc anode with and without nano-$CaCO_3$ during Zn stripping/plating cycling (ref. [141]).

Inorganic coatings

Several inorganic materials have been demonstrated to be promising for modifying the surface characteristics of the Zn electrode. Lee et al.[139,140] showed that Zn powders coated by aluminum oxide (Al_2O_3) and bismuth oxide (Bi_2O_3) via a facile chemical solution process could effectively suppress the competitive H_2 evolution in an alkaline electrolyte. Reduced graphene oxide and porous nano-$CaCO_3$ (Fig. 16) were found to improve the stripping/plating stability of Zn anodes and depress Zn dendrite growth[141]. Currently, atomic layer deposition (ALD) has been developed as a special coating method that can achieve excellent coverage, conformal deposition and precisely controllable film thickness at the nanoscale level. With the ALD method, an ultrathin TiO_2 coating layer for a Zn anode was prepared successfully, which significantly suppressed Zn corrosion and gas evolution[142].

The formation of passivation byproducts (ZnO) is another reason for the irreversibility of ZB systems. To improve the rechargeability, a Bi_2O_3-ZnO-CaO coating layer with the ability to capture zincate ions was adopted to prevent supersaturation at the anode and the formation of passive layers, enabling a cyclic stability of 20 full cycles in excess electrolyte, whereas bare Zn fulfilled just one complete discharge[140]. It was also reported that the Zn anode coated with a SiO_2 layer through a chemical solution process showed an increased Zn utilization, at least 5% higher than that of the uncoated Zn anode at C/20 rate, and enabled recharging even after undergoing 100% DOD_{Zn}[143].

Structure design of Zn electrodes

In commercial ZBs, the Zn anodes generally comprise a gelled mixture of granulated Zn powders with large particle sizes in the range of 50–200 mesh[6], while in laboratory research, polished Zn foil is most frequently used[144,145]. Both granulated Zn powders and Zn foil are cost-effective for industrial production. However, Zn particles with high surface areas are more favorable for better electrochemical performance of ZBs as the electrode-electrolyte contact interface area increases.

Three-dimensional Zn electrodes

In addition to metallic Zn anodes in foil and powder forms, various nanostructured Zn electrodes with high surface areas have been proposed to improve the electrochemical performance of ZBs[146–148]. Parker et al.[147] created a Ni/Zn battery with a sponge Zn anode instead of powdered Zn. This monolithic three-dimensional (3D) Zn anode can be cycled hundreds to thousands of times without undergoing passivation or macro-dendrite formation (Fig. 17). Further studies indicated that electric currents are more uniformly distributed within the

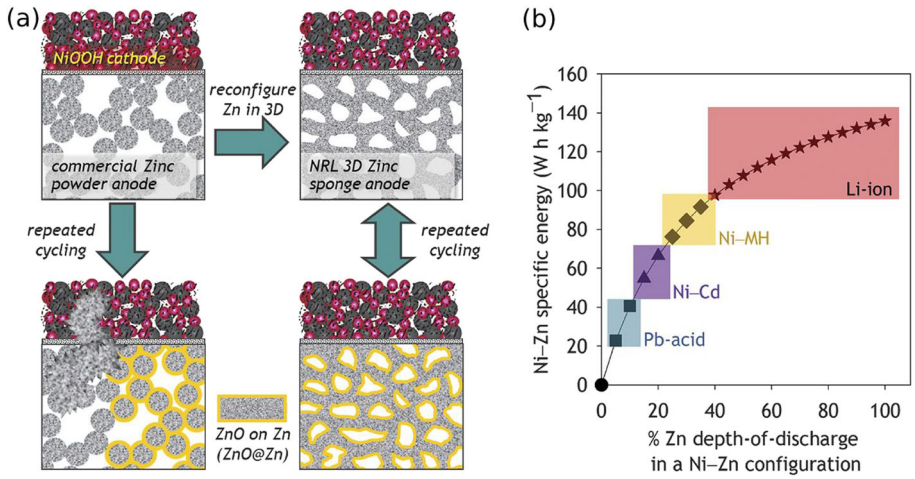

Fig. 17 Illustrations of rechargeable Ni/Zn batteries. a Comparison of the cycling processes of Ni/Zn batteries adopting conventional powder Zn anodes versus 3D Zn with a monolithic aperiodic sponge morphology. **b** The estimated specific energy of a fully packaged Ni/Zn cell with different Zn depths of discharge versus a capacity-matched NiOOH electrode. The shaded areas represent the specific energy range of common battery chemistries (ref. [147]).

sponge skeleton, making it physically difficult to form dendrites. In addition, the cells reached an average of 91% depth of discharge (DOD_{Zn}) and could be recharged to >95% capacity from these extreme depths at a current density of 10 mA cm^{-2}. The corresponding energy density is even comparable with those of typical LIBs.

Zhang et al.[15] introduced fibrous Zn electrodes for applications in large-size alkaline ZBs. The solid fibrous Zn anode was found to have good physical stability and connectivity among individual fibers, ensuring good electrical conductivity, mechanical stability, and design flexibility for controlling mass distribution, porosity and effective surface area. Such anodes could provide 20% more capacity in alkaline cells at high discharging currents compared to that of commercially available cells. However, as the surface area increased for 3D electrodes, the Zn corrosion became more severe, which would consume electrolyte and result in the loss of active Zn[149].

Carbon-based substrates

The inherent excellent electrical conductivity and open structure of carbon materials enable uniform Zn deposition[150]. Li et al.[151] proposed that the composite Zn anodes prepared by mixing Zn particles with activated carbon (AC) had a smaller tendency for the formation of inactive Zn sulfates that could inhibit the Zn deposition/dissolution. Moreover, with increasing AC ratio, Zn dendrite growth was suppressed (Fig. 18a–d) because of the rich accommodation sites for Zn deposition provided by the AC particles. The N_2 adsorption/desorption isotherms and density function theory analyses showed the disappearance of micropores of AC, clarifying that the deposition of Zn dendrites and the formation of other products occurred in the pores of AC (Fig. 18f). When tested in Zn/α-MnO_2 cells with aqueous $ZnSO_4$ electrolytes, the composite anode containing 12 wt% AC exhibited a capacity retention of 85.6% (initial capacity of ~ 170 mA g^{-1}) at a current density of 200 mA g^{-1} after 80 cycles (Fig. 18e).

Wang et al.[152] electrodeposited Zn on carbon fibers (CFs) to fabricate Zn@CF anodes with a core-shell structure. The Zn@CF//Co_3O_4 battery suffered only 20% capacity decay after 2000 full cycles, while the battery with a Zn plate failed to work after only 900 cycles. By virtue of the core-shell feature, the Zn@CF anode featured a large specific area, which facilitated electrochemical kinetics and improved the reversibility of the Zn/Zn^{2+} redox couple. Importantly, no Zn dendrite was detected on the Zn@CF electrode even after 2000 cycles. Ma et al.[153] further confirmed the positive effects on Zn electrochemistry provided by the carbon matrix. In their study, a Zn-carbon cloth electrode was prepared by a facile electrochemical deposition method using a two-electrode setup. Based on this carbon-assisted anode, the aqueous Zn/Co_3O_4 battery delivered a high voltage of 2.2 V, a capacity of 205 mA h g^{-1} and an extremely high cycling stability with 92% capacity retention after 5000 cycles.

Conclusions and perspectives

Research on ZBs has been revived by global burgeoning demands for safe and environmentally friendly electrochemical energy storage systems. To date, reliable secondary ZBs that can be competitive with prevailing

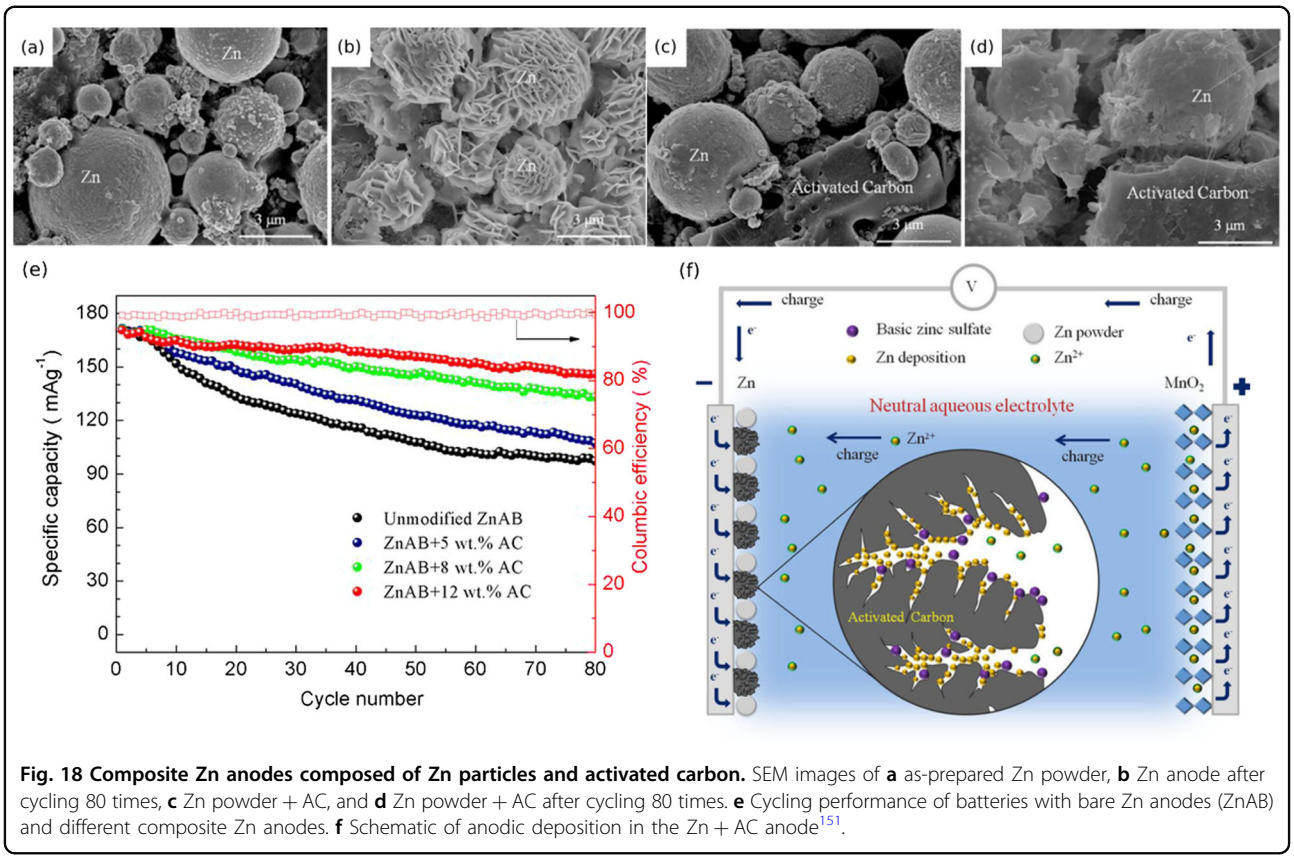

Fig. 18 Composite Zn anodes composed of Zn particles and activated carbon. SEM images of **a** as-prepared Zn powder, **b** Zn anode after cycling 80 times, **c** Zn powder + AC, and **d** Zn powder + AC after cycling 80 times. **e** Cycling performance of batteries with bare Zn anodes (ZnAB) and different composite Zn anodes. **f** Schematic of anodic deposition in the Zn + AC anode[151].

LIBs and lead-acid batteries are still lacking. The development of Zn anodes with noncorroding and uniform deposition/dissolution properties is the key to achieving long cycling life and high CE in ZBs. It is therefore of great importance to break the routine of classical configurations involving ordinary aqueous electrolytes and untreated Zn metallic anodes. In this review, the fundamentals and recent works addressing critical issues have been highlighted, with an emphasis on novel electrolyte systems (including compatible solvents, stable Zn salts, and additives), interphase construction and anode structure design. Despite promising progress over the past 5 years, many aspects associated with the interface reactions of metallic Zn anodes are not fully understood and will require additional investigations, especially when compared with the wealth of knowledge regarding battery systems based on typical alkali and alkaline metals.

Notably, the major developments in reliable rechargeable Zn anodes and their objective evaluation have been mainly hindered by the limited availability of appropriate electrolytes. Although liquid-like electrolyte systems can facilitate desirable electrochemical performance of ZBs on a laboratory scale, their further practical application still faces obstacles including dendrite formation, electrolyte leakage, and flammability. WiSEs can significantly expand the wide electrochemical window of aqueous electrolytes, suppress undesired side reactions and inhibit Zn dendrite growth. However, due to the high cost of metal salts, high viscosity and sacrificed energy density, alternative cost-effective electrolyte systems with desirable (electro)chemical properties and specific interface structures are particularly required.

The application of polymer electrolytes has overwhelming advantages, such as the inhibition of Zn corrosion and dendrite growth and good processability. As shown in Table 3, $Zn(CF_3SO_3)_2$ has been the most extensively applied dopant salt in polymer electrolytes due to its relatively low cost and high ion conductivity. Among all the SPEs and GPEs, the electrolytes prepared with PVdF-HFP doped with inorganic mineral fillers consistently exhibit top-level ion conductivity, suggesting their merit as future electrolyte candidates in rechargeable ZBs. Although the ion conductivities of most GPEs could be maintained at a magnitude of 1 mS cm^{-1}, normally 10-fold higher than that of SPE samples (Table 3), the ion transference number needs to be further optimized. Enlightened by the >0.9 Li^+ ion transference number of SCC systems from LIBs, the development of novel SCC-based polymer systems with

Table 3 Summary of polymer electrolytes for Zn^{2+} transportation.

Electrolyte type	Matrix	Salt	Plasticizer	Ion conductivity at r.t. or 30 °C (mS/cm)	Transference number	Ref.
SPE	PEO	$ZnCl_2$	NA	$\sim 3 \times 10^{-6}$	NA	73
	PEO	$ZnBr_2$		$\sim 7 \times 10^{-6}$		73
	PEO	ZnI_2		$\sim 7 \times 10^{-6}$		73
	PEO[a]	$Zn(CH_3COO)_2$		1.6×10^{-3}		74
	PEO [b]	$Zn(CH_3COO)_2$		1.2×10^{-4}	0.17	75
	PEO	$Zn(CF_3SO_3)_2$		1.1×10^{-3}	0.17	76
	PEO/PVdF	$Zn(CF_3SO_3)_2$		2.5×10^{-2}	NA	86
	Di-urea crosslinked PEO containing siloxance ormolytes	$Zn(CF_3SO_3)_2$		3×10^{-3}		78
	PEO/PPG incorporated with Al_2O_3	$Zn(CF_3SO_3)_2$		2.1×10^{-2}		79
	γ-irradiation crosslinked PEO incorporated with TiO_2	$ZnCl_2$		$\sim 1 \times 10^{-1}$		80
	PEO incorporated with Kevlar nanofibers	$Zn(CF_3SO_3)_2$		2.5×10^{-2}		83
	PVdF-HFP incorporated with ZrO_2	$Zn(CF_3SO_3)_2$		4.6×10^{-1}		81
	PVdF-HFP incorporated with TiO_2	$Zn(CF_3SO_3)_2$		3.4×10^{-1}	0.57	102
	PVC/PEMA	$Zn(CF_3SO_3)_2$		2.8×10^{-3}	0.56	114
GPE	PEO/PVdF	$Zn(CF_3SO_3)_2$	[EMIM][TFSI]	1.6×10^{-1}	NA	86
	PEO-poly(propylene oxide) - PEO	$Li_2SO_4/ZnSO_4$	Water	6.3		84
	PVdF-HFP	$Zn(TFSI)_2$	[EMI][TFSI]/EC/PEGDME	4.7×10^{-1}		85
	PVdF-HFP	$Zn(TFSI)_2$	$[EMI][CF_3SO_3]$	1.1		164
	PVdF-HFP	$Zn(CF_3SO_3)_2$	$[EMI][CF_3SO_3]$	1.3		164
	PVdF-HFP incorporated with ZnO	$Zn(CF_3SO_3)_2$	EC/PC	6.7	0.55	104
	PVdF-HFP	$Zn(CF_3SO_3)_2$	$[EMI][CF_3SO_3]$/NMP	7.1	NA	105
	PVdF-HFP	$Zn(CF_3SO_3)_2$	$[EMI][CF_3SO_3]$/NMP	3.8	0.30	105
	PVC/PEMA	$Zn(CF_3SO_3)_2$	[EMIM][TFSI]	1.1×10^{-1}	0.63	113,114
	PVC/PEMA incorporated with SiO_2	$Zn(CF_3SO_3)_2$	[EMIM][TFSI]	6.7×10^{-1}	0.69	82
	PAN-S	NA	Water	8.1×10^{-2}	NA	120

[a]Electrolyte prepared by solution casting method
[b]Electrolyte prepared by hot-press casting method

unusual improvements in both the rate and efficacy of Zn^{2+} transport can possibly provide alternative approaches to solve the challenges faced by Zn electrolytes and ZBs.

Acknowledgements
This work was supported by the Programs of the National Natural Science Foundation of China (Grant Nos. 21601195 and 51625204), the Strategic Priority Research Program of the Chinese Academy of Sciences (XDA22010600), and the National Key R&D Program of China (Grant No.

2018YFB0104300). J. Zhao particularly appreciates the financial aid from the Youth Innovation Promotion Association of Chinese Academy of Sciences (2019214).

Author details
[1]Qingdao Industrial Energy Storage Research Institute, Qingdao Institute of Bioenergy and Bioprocess Technology, Chinese Academy of Sciences, Qingdao 266101, China. [2]College of Chemistry and Molecular Engineering, Qingdao University of Science and Technology, Qingdao 266042, China. [3]School of Polymer Science and Engineering, Qingdao University of Science and Technology, Qingdao 266042, China

Conflict of interest
The authors declare that they have no conflict of interest.

Received: 2 June 2019 Revised: 31 July 2019 Accepted: 27 August 2019. Published online: 24 January 2020

References

1. Liu, Z. et al. Three-dimensional ordered porous electrode materials for electrochemical energy storage. *NPG Asia Mater.* **11**, 12 (2019).
2. Zhang, P., Zhao, Y. & Zhang, X. Functional and stability orientation synthesis of materials and structures in aprotic Li-O_2 batteries. *Chem. Soc. Rev.* **47**, 2921–3004 (2018).
3. Xie, J. & Zhang, Q. Recent progress in multivalent metal (Mg, Zn, Ca, and Al) and metal-ion rechargeable batteries with organic materials as promising electrodes. *Small* **15**, 1805061 (2019).
4. Song, M., Tan, H., Chao, D. L. & Fan, H. J. Recent advances in Zn-ion batteries. *Adv. Funct. Mater.* **28**, 1802564 (2018).
5. Wang, F. et al. Nanostructured positive electrode materials for post-lithium ion batteries. *Energ. Environ. Sci.* **9**, 3570–3611 (2016).
6. Li, Y. & Dai, H. Recent advances in zinc-air batteries. *Chem. Soc. Rev.* **43**, 5257–5275 (2014).
7. Hoang, T. K., Sun, K. E. K. & Chen, P. Corrosion chemistry and protection of zinc & zinc alloys by polymer-containing materials for potential use in rechargeable aqueous batteries. *RSC Adv.* **5**, 41677–41691 (2015).
8. Chen, X. et al. Recent advances in materials and design of electrochemically rechargeable zinc-air batteries. *Small* **14**, 1801929 (2018).
9. Konarov, A. et al. Present and future perspective on electrode materials for rechargeable zinc-ion batteries. *ACS Energy Lett.* **3**, 2620–2640 (2018).
10. Lu, W., Xie, C., Zhang, H. & Li, X. Inhibition of zinc dendrite growth in zinc-based batteries. *ChemSusChem* **11**, 3996–4006 (2018).
11. Wang, F. et al. Highly reversible zinc metal anode for aqueous batteries. *Nat. Mater.* **17**, 543–549 (2018).
12. Han, S. D. et al. Origin of electrochemical, structural, and transport properties in nonaqueous zinc electrolytes. *ACS Appl. Mater. Interfaces* **8**, 3021–3031 (2016).
13. Suo, L. M. et al. "Water-in-salt" electrolyte enables high-voltage aqueous lithium-ion chemistries. *Science* **350**, 938–943 (2015).
14. Zhao, J. W. et al. High-voltage Zn/$LiMn_{0.8}Fe_{0.2}PO_4$ aqueous rechargeable battery by virtue of "water-in-salt" electrolyte. *Electrochem. Commun.* **69**, 6–10 (2016).
15. Zhang, N. et al. Cation-deficient spinel $ZnMn_2O_4$ cathode in $Zn(CF_3SO_3)_2$ electrolyte for rechargeable aqueous Zn-ion battery. *J. Am. Chem. Soc.* **138**, 12894–12901 (2016).
16. Mylius, F. & Dietz, R. Zinc-chloride (studies into the solubility of salt XIV). *Z. Anorg. Chem.* **44**, 209–220 (1905).
17. Zhang, C. et al. A $ZnCl_2$ water-in-salt electrolyte for a reversible Zn metal anode. *Chem. Commun.* **54**, 14097–14099 (2018).
18. Chen, C. Y., Matsumoto, K., Kubota, K., Hagiwara, R. & Xu, Q. A room-temperature molten hydrate electrolyte for rechargeable zinc-air batteries. *Adv. Energy Mater.* **9**, 1900196 (2019).
19. Fang, G. Z., Zhou, J., Pan, A. Q. & Liang, S. Q. Recent advances in aqueous zinc-ion batteries. *ACS Energy Lett.* **3**, 2480–2501 (2018).
20. Naveed, A., Yang, H. J., Yang, J., Nuli, Y. N. & Wang, J. L. Highly reversible and rechargeable safe Zn batteries based on a triethyl phosphate electrolyte. *Angew. Chem. Int. Ed.* **58**, 2760–2764 (2019).
21. Kundu, D. et al. Aqueous vs. nonaqueous Zn-ion batteries: consequences of the desolvation penalty at the interface. *Energ. Environ. Sci.* **11**, 881–892 (2018).
22. Earle, M. J. & Seddon, K. R. Green solvents for the future. *Pure Appl. Chem.* **72**, 1391–1398 (2000).
23. Quinn, B. M., Ding, Z., Moulton, R. & Bard, A. J. Novel electrochemical studies of ionic liquids. *Langmuir* **18**, 1734–1742 (2002).
24. Armand, M., Endres, F., MacFarlane, D. R., Ohno, H. & Scrosati, B. *Materials for sustainable energy: a collection of peer-reviewed research and review articles from nature publishing group*. (World Scientific, Ltd., Singapore, 2011).
25. Chen, P.-Y. & Hussey, C. L. The electrodeposition of Mn and Zn-Mn alloys from the room-temperature tri-1-butylmethylammonium bis (trifluoromethane sulfonyl) imide ionic liquid. *Electrochim. Acta* **52**, 1857–1864 (2007).
26. Kar, M., Winther-Jensen, B., Forsyth, M. & MacFarlane, D. R. Chelating ionic liquids for reversible zinc electrochemistry. *Phys. Chem. Chem. Phys.* **15**, 7191–7197 (2013).
27. Doan, N., Vainikka, T., Rautama, E.-L., Kontturi, K. & Johans, C. Electrodeposition of macroporous Zn and ZnO films from ionic liquids. *Int. J. Electrochem. Sci.* **7**, 12034–12044 (2012).
28. Tulodziecki, M., Tarascon, J.-M., Taberna, P.-L. & Guéry, C. Electrodeposition growth of oriented ZnO deposits in ionic liquid media. *J. Electrochem. Soc.* **159**, D691–D698 (2012).
29. Azaceta, E. et al. Electrochemical deposition of ZnO in a room temperature ionic liquid: 1-butyl-1-methylpyrrolidinium bis (trifluoromethane sulfonyl) imide. *Electrochem. Commun.* **11**, 2184–2186 (2009).
30. Ghazvini, M. S. et al. Electrodeposition and stripping behavior of a zinc/polystyrene composite electrode in an ionic liquid. *J. Solid State Electrochem.* **19**, 1453–1461 (2015).
31. Steichen, M., Brooks, N. R., Van Meervelt, L., Fransaer, J. & Binnemans, K. Homoleptic and heteroleptic N-alkylimidazole zinc(II)-containing ionic liquids for high current density electrodeposition. *Dalton Trans.* **43**, 12329–12341 (2014).
32. Simons, T. J. et al. Influence of Zn^{2+} and water on the transport properties of a pyrrolidinium dicyanamide ionic liquid. *J. Phys. Chem. B* **118**, 4895–4905 (2014).
33. Simons, T., Torriero, A., Howlett, P., MacFarlane, D. & Forsyth, M. High current density, efficient cycling of Zn^{2+} in 1-ethyl-3-methylimidazolium dicyanamide ionic liquid: the effect of Zn^{2+} salt and water concentration. *Electrochem. Commun.* **18**, 119–122 (2012).
34. Xu, M., Ivey, D., Xie, Z. & Qu, W. Electrochemical behavior of Zn/Zn(II) couples in aprotic ionic liquids based on pyrrolidinium and imidazolium cations and bis (trifluoromethanesulfonyl) imide and dicyanamide anions. *Electrochim. Acta* **89**, 756–762 (2013).
35. Deng, M.-J., Lin, P.-C., Chang, J.-K., Chen, J.-M. & Lu, K.-T. Electrochemistry of Zn (II)/Zn on Mg alloy from the N-butyl-N-methylpyrrolidinium dicyanamide ionic liquid. *Electrochim. Acta* **56**, 6071–6077 (2011).
36. Simons, T. J., MacFarlane, D. R., Forsyth, M. & Howlett, P. C. Zn electrochemistry in 1-ethyl-3-methylimidazolium and n-butyl-n-methylpyrrolidinium dicyanamides: promising new rechargeable Zn battery electrolytes. *ChemElectroChem* **1**, 1688–1697 (2014).
37. Liu, Z., El Abedin, S. Z. & Endres, F. Electrodeposition of zinc films from ionic liquids and ionic liquid/water mixtures. *Electrochim. Acta* **89**, 635–643 (2013).
38. Bayer, M. et al. Influence of water content on the surface morphology of zinc deposited from EMImOTf/water mixtures. *J. Electrochem. Soc.* **166**, A909–A914 (2019).
39. Xu, M., Ivey, D., Xie, Z., Qu, W. & Dy, E. The state of water in 1-butly-1-methylpyrrolidinium bis (trifluoromethanesulfonyl) imide and its effect on Zn/Zn(II) redox behavior. *Electrochim. Acta* **97**, 289–295 (2013).
40. Simons, T., Howlett, P., Torriero, A., MacFarlane, D. & Forsyth, M. Electrochemical, transport, and spectroscopic properties of 1-ethyl-3-methylimidazolium ionic liquid electrolytes containing zinc dicyanamide. *J. Phys. Chem. C.* **117**, 2662–2669 (2013).
41. Xu, M., Ivey, D., Qu, W. & Xie, Z. Improved Zn/Zn(II) redox kinetics, reversibility and cyclability in 1-ethyl-3-methylimmidazolium

dicyanamide with water and dimethyl sulfoxide added. *J. Power Sources* **252**, 327–332 (2014).
42. Dilasari, B., Jung, Y. & Kwon, K. Effect of water on the stability of zinc in 1-butyl-1-methylpyrrolidinium bis (trifluoromethylsulfonyl) imide ionic liquid. *J. Ind. Eng. Chem.* **45**, 375–379 (2017).
43. Periyapperuma, K., Pozo-Gonzalo, C., MacFarlane, D. R., Forsyth, M. & Howlett, P. C. High Zn concentration pyrrolidinium-dicyanamide-based ionic liquid electrolytes for Zn^{2+}/Zn^{0} electrochemistry in a flow environment. *ACS Appl. Energy Mater.* **1**, 4580–4590 (2018).
44. Kar, M. et al. Stable zinc cycling in novel alkoxy-ammonium based ionic liquid electrolytes. *Electrochim. Acta* **188**, 461–471 (2016).
45. Liu, Z. et al. Dendrite-free nanocrystalline zinc electrodeposition from an ionic liquid containing nickel triflate for rechargeable Zn-based batteries. *Angew. Chem. Int. Ed.* **55**, 2889–2893 (2016).
46. Liu, Z., El Abedin, S. Z. & Endres, F. Raman and FTIR spectroscopic studies of 1-ethyl-3-methylimidazolium trifluoromethylsulfonate, its mixtures with water and the solvation of zinc ions. *ChemPhysChem* **16**, 970–977 (2015).
47. Abbott, A. P., Capper, G., Davies, D. L., Rasheed, R. K. & Tambyrajah, V. Novel ambient temperature ionic liquids for zinc and zinc alloy electrodeposition. *Trans. IMF* **79**, 204–206 (2001).
48. Chen, Y.-H. et al. Electrodeposition of compact zinc from the hydrophobic Brønsted acidic ionic liquid-based electrolytes and the study of zinc stability along with the acidity manipulation. *Electrochim. Acta* **227**, 185–193 (2017).
49. Abbott, A. P., Ryder, K. & König, U. Electrofinishing of metals using eutectic based ionic liquids. *Trans. IMF* **86**, 196–204 (2008).
50. Zhang, Q., Vigier, K. D. O., Royer, S. & Jérôme, F. Deep eutectic solvents: syntheses, properties and applications. *Chem. Soc. Rev.* **41**, 7108–7146 (2012).
51. Smith, E. L., Abbott, A. P. & Ryder, K. S. Deep eutectic solvents (DESs) and their applications. *Chem. Rev.* **114**, 11060–11082 (2014).
52. Abbott, A. P., Harris, R. C. & Ryder, K. S. Application of hole theory to define ionic liquids by their transport properties. *J. Phys. Chem. B* **111**, 4910–4913 (2007).
53. Abbott, A. P. Model for the conductivity of ionic liquids based on an infinite dilution of holes. *ChemPhysChem* **6**, 2502–2505 (2005).
54. Abbott, A. P., Capper, G., Davies, D. L., Rasheed, R. K. & Tambyrajah, V. Novel solvent properties of choline chloride/urea mixtures. *Chem. Commun.* **9**, 70–71 (2003).
55. Abbott, A. P. et al. Double layer effects on metal nucleation in deep eutectic solvents. *Phys. Chem. Chem. Phys.* **13**, 10224–10231 (2011).
56. Zhao, J. et al. "Water-in-deep eutectic solvent" electrolytes enable zinc metal anodes for rechargeable aqueous batteries. *Nano Energy* **57**, 625–634 (2019).
57. Abbott, A. P., Capper, G., Davies, D. L., Rasheed, R. K. & Shikotra, P. Selective extraction of metals from mixed oxide matrixes using choline-based ionic liquids. *Inorg. Chem.* **44**, 6497–6499 (2005).
58. Zhang, J. et al. Amide-based molten electrolyte with hybrid active ions for rechargeable Zn batteries. *Electrochim. Acta* **280**, 108–113 (2018).
59. Narayanan, N. V., Ashokraj, B. & Sampath, S. Physicochemical, electrochemical, and spectroscopic characterization of zinc-based room-temperature molten electrolytes and their application in rechargeable batteries. *J. Electrochem. Soc.* **156**, A863–A872 (2009).
60. Narayanan, N. V., Ashokraj, B. & Sampath, S. Ambient temperature, zinc ion-conducting, binary molten electrolyte based on acetamide and zinc perchlorate: application in rechargeable zinc batteries. *J. Colloid Interface Sci.* **342**, 505–512 (2010).
61. Tan, P. et al. Flexible Zn- and Li-air batteries: recent advances, challenges, and future perspectives. *Energ. Environ. Sci.* **10**, 2056–2080 (2017).
62. Song, J., Wang, Y. & Wan, C. C. Review of gel-type polymer electrolytes for lithium-ion batteries. *J. Power Sources* **77**, 183–197 (1999).
63. Meyer, W. H. Polymer electrolytes for lithium-ion batteries. *Adv. Mater.* **10**, 439–448 (1998).
64. Xu, M., Ivey, D., Xie, Z. & Qu, W. Rechargeable Zn-air batteries: progress in electrolyte development and cell configuration advancement. *J. Power Sources* **283**, 358–371 (2015).
65. Zhang, Q., Liu, K., Ding, F. & Liu, X. Recent advances in solid polymer electrolytes for lithium batteries. *Nano Res.* **10**, 4139–4174 (2017).
66. Lopez, J., Mackanic, D. G., Cui, Y. & Bao, Z. Designing polymers for advanced battery chemistries. *Nat. Rev. Mater.* **4**, 312–330 (2019).
67. Ni'mah, Y. L., Cheng, M.-Y., Cheng, J. H., Rick, J. & Hwang, B.-J. Solid-state polymer nanocomposite electrolyte of TiO_2/PEO/$NaClO_4$ for sodium ion batteries. *J. Power Sources* **278**, 375–381 (2015).
68. Mainar, A. R. et al. An overview of progress in electrolytes for secondary zinc-air batteries and other storage systems based on zinc. *J. Energy Storage* **15**, 304–328 (2018).
69. Patrick, A., Glasse, M., Latham, R. & Linford, R. Novel solid state polymeric batteries. *Solid State Ion.* **18**, 1063–1067 (1986).
70. Plancha, M., Rangel, C. & Sequeira, C. Pseudo-equilibrium phase diagrams for PEO-Zn salts-based electrolytes. *Solid State Ion.* **116**, 293–300 (1999).
71. Glasse, M. D., Linford, R. G., & Schlindwein, W. S. *Proc. Second Int. Symposium on Polymer Electrolytes* **203** (1989).
72. Staunton, E. et al. Structure of the poly (ethylene oxide)-zinc chloride complex. *Angew. Chem. Int. Ed.* **43**, 2103–2105 (2004).
73. Yang, H. & Farrington, G. Poly (ethylene oxide)-based Zn(II) halide electrolytes. *J. Electrochem. Soc.* **139**, 1646–1654 (1992).
74. Polu, A. R., Kumar, R. & Joshi, G. M. Effect of zinc salt on transport, structural, and thermal properties of PEG-based polymer electrolytes for battery application. *Ionics* **20**, 675–679 (2014).
75. Karan, S., Sahu, T. B., Sahu, M. & Agrawal, R. Investigations on ion transport behaviour in a non-lithium chemical based solid polymer electrolyte (SPE): [PEO:ZnA]. *Mater. Today.: Proc.* **3**, 109–114 (2016).
76. Karan, S., Sahu, T. B., Sahu, M., Mahipal, Y. & Agrawal, R. Characterization of ion transport property in hot-press cast solid polymer electrolyte (SPE) films:[PEO: $Zn(CF_3SO_3)_2$]. *Ionics* **23**, 2721–2726 (2017).
77. Frank Frederick, C. & Tosi, M. On the theory of polymer crystallization. *Proc. R. Soc. Lond., Ser. A* **263**, 323–339 (1961).
78. Nunes, S. et al. Study of sol-gel derived di-ureasils doped with zinc triflate. *Solid State Sci.* **8**, 1484–1491 (2006).
79. Nancy, A. C. & Suthanthiraraj, S. A. Effect of Al_2O_3 nanofiller on the electrical, thermal and structural properties of PEO: PPG based nanocomposite polymer electrolyte. *Ionics* **23**, 1439–1449 (2017).
80. Pucić, I. & Turković, A. Radiation modification of $(PEO)_8ZnCl_2$ polyelectrolyte and nanocomposite. *Solid State Ion.* **176**, 1797–1800 (2005).
81. Johnsi, M. & Suthanthiraraj, S. A. Compositional effect of ZrO_2 nanofillers on a PVDF-co-HFP based polymer electrolyte system for solid state zinc batteries. *Chin. J. Polym. Sci.* **34**, 332–343 (2016).
82. Candhadai Murali, S. P. & Samuel, A. S. Zinc ion conducting blended polymer electrolytes based on room temperature ionic liquid and ceramic filler. *J. Appl. Polym. Sci.*, **136**, 47654 (2019).
83. Wang, M. et al. Biomimetic solid-state Zn^{2+} electrolyte for corrugated structural batteries. *ACS Nano.* **13**, 1107—1115 (2019).
84. Zhao, J. et al. A smart flexible zinc battery with cooling recovery ability. *Angew. Chem.* **129**, 7979–7983 (2017).
85. Ye, H. & Xu, J. J. Zinc ion conducting polymer electrolytes based on oligomeric polyether/PVDF-HFP blends. *J. Power Sources* **165**, 500–508 (2007).
86. Rathika, R., Padmaraj, O. & Suthanthiraraj, S. A. Electrical conductivity and dielectric relaxation behaviour of PEO/PVdF-based solid polymer blend electrolytes for zinc battery applications. *J. Mater. Sci.: Mater. Electron.* **24**, 243–255 (2018).
87. Fauvarque, J. F., Guinot, S., Bouzir, N., Salmon, E. & Penneau, J. F. Alkaline poly (ethylene oxide) solid polymer electrolytes. Application to nickel secondary batteries. *Electrochim. Acta* **40**, 2449–2453 (1995).
88. Guinot, S., Salmon, E., Penneau, J. & Fauvarque, J. A new class of PEO-based SPEs: structure, conductivity and application to alkaline secondary batteries. *Electrochim. Acta* **43**, 1163–1170 (1998).
89. Vassal, N., Salmon, E. & Fauvarque, J. F. Electrochemical properties of an alkaline solid polymer electrolyte based on P(ECH-co-EO). *Electrochim. Acta* **45**, 1527–1532 (2000).
90. Wang, K. et al. High-performance cable-type flexible rechargeable Zn battery based on MnO_2@CNT fiber microelectrode. *ACS Appl. Mater. Interfaces* **10**, 24573–24582 (2018).
91. Mohamad, A. et al. Ionic conductivity studies of poly (vinyl alcohol) alkaline solid polymer electrolyte and its use in nickel-zinc cells. *Solid State Ion.* **156**, 171–177 (2003).
92. Vatsalarani, J., Kalaiselvi, N. & Karthikeyan, R. Effect of mixed cations in synergizing the performance characteristics of PVA-based polymer electrolytes for novel category Zn/AgO polymer batteries-a preliminary study. *Ionics* **15**, 97–105 (2009).
93. Yang, C.-C., Lin, S.-J. & Hsu, S.-T. Synthesis and characterization of alkaline polyvinyl alcohol and poly (epichlorohydrin) blend polymer electrolytes and performance in electrochemical cells. *J. Power Sources* **122**, 210–218 (2003).

94. Xu, Y. et al. Flexible, stretchable, and rechargeable fiber-shaped zinc-air battery based on cross-stacked carbon nanotube sheets. *Angew. Chem. Int. Ed.* **54**, 15390–15394 (2015).
95. Zeng, Y. et al. An ultrastable and high-performance flexible fiber-shaped Ni-Zn battery based on a Ni-NiO heterostructured nanosheet cathode. *Adv. Mater.* **29**, 1702698 (2017).
96. Fan, X. et al. Porous nanocomposite gel polymer electrolyte with high ionic conductivity and superior electrolyte retention capability for long-cycle-life flexible zinc-air batteries. *Nano Energy* **56**, 454–462 (2019).
97. Yang, S., Bo, M., Peng, C., Li, Y. & Li, Y. Three-electrode flexible zinc-nickel battery with black phosphorus modified polymer electrolyte. *Mater. Lett.* **233**, 118–121 (2018).
98. Fu, J. et al. Flexible High-energy polymer-electrolyte-based rechargeable zinc-air batteries. *Adv. Mater.* **27**, 5617–5622 (2015).
99. Zamarayeva, A. M. et al. Fabrication of a high-performance flexible silver-zinc wire battery. *Adv. Electron. Mater.* **2**, 1500296 (2016).
100. Rathika, R. & Suthanthiraraj, S. A. Influence of 1-ethyl-3-methylimidazolium bis (trifluoromethyl sulfonyl) imide plasticization on zinc-ion conducting PEO/PVdF blend gel polymer electrolyte. *J. Mater. Sci.: Mater. Electron.* **29**, 19632–19643 (2018).
101. Johnsi, M. & Suthanthiraraj, S. A. Electrochemical and structural properties of a polymer electrolyte system based on the effect of CeO_2 nanofiller with PVDF-co-HFP for energy storage devices. *Ionics* **22**, 1075–1083 (2016).
102. Johnsi, M. & Suthanthiraraj, S. A. Preparation, zinc ion transport properties, and battery application based on poly (vinilydene fluoride-co-hexa fluoro propylene) polymer electrolyte system containing titanium dioxide nanofiller. *High. Perform. Polym.* **27**, 877–885 (2015).
103. Tafur, J. P. & Fernández Romero, A. J. Electrical and spectroscopic characterization of PVdF-HFP and TFSI-ionic liquids-based gel polymer electrolyte membranes. Influence of $ZnTf_2$ salt. *J. Mater. Sci.* **469**, 499–506 (2014).
104. Sellam & Hashmi, S. Enhanced zinc ion transport in gel polymer electrolyte: effect of nano-sized ZnO dispersion. *J. Solid State Electrochem.* **16**, 3105–3114 (2012)..
105. Tafur, J., Santos, F. & Romero, A. Influence of the ionic liquid type on the gel polymer electrolytes properties. *Membranes* **5**, 752–771 (2015).
106. Guisao, J. P. T. & Romero, A. J. F. Interaction between Zn^{2+} cations and n-methyl-2-pyrrolidone in ionic liquid-based Gel Polymer Electrolytes for Zn batteries. *Electrochim. Acta* **176**, 1447–1453 (2015).
107. Wang, Z. et al. Hydrogel electrolytes for flexible aqueous energy storage devices. *Adv. Funct. Mater.* **28**, 1804560 (2018).
108. Wu, G., Lin, S. & Yang, C. Alkaline Zn-air and Al-air cells based on novel solid PVA/PAA polymer electrolyte membranes. *J. Membr. Sci.* **280**, 802–808 (2006).
109. Chaduang, S., Lao-atiman, W. & Kheawhom, S. Improving performance and cyclability of printed flexible zinc-air batteries using carbopol gel electrolyte. *ECS Trans.* **77**, 55–62 (2017).
110. Huang, Y. et al. Solid-state rechargeable Zn//NiCo and Zn-air batteries with ultralong lifetime and high capacity: the role of a sodium polyacrylate hydrogel electrolyte. *Adv. Energy Mater.* **8**, 1802288 (2018).
111. Liu, J. et al. An intrinsically 400% stretchable and 50% compressible NiCo//Zn battery. *Nano Energy* **58**, 338–346 (2019).
112. Ma, L. et al. Super-stretchable zinc-air batteries based on an alkaline-tolerant dual-network hydrogel electrolyte. *Adv. Energy Mater.* **9**, 1803046 (2019).
113. Prasanna, C. S. & Suthanthiraraj, S. A. Effective influences of 1-ethyl-3-methylimidazolium bis (trifluoromethylsulfonyl) imide (EMIMTFSI) ionic liquid on the ion transport properties of micro-porous zinc-ion conducting poly (vinyl chloride)/poly (ethyl methacrylate) blend-based polymer electrolytes. *J. Polym. Res.* **23**, 140 (2016).
114. Prasanna, C. M. S. & Suthanthiraraj, S. A. Dielectric and thermal features of zinc ion conducting gel polymer electrolytes (GPEs) containing PVC/PEMA blend and EMIMTFSI ionic liquid. *Ionics* **24**, 2631–2646 (2018).
115. Tan, M. J. et al. Acrylamide-derived freestanding polymer gel electrolyte for flexible metal-air batteries. *J. Power Sources* **400**, 566–571 (2018).
116. Lee, S.-H., Kim, K. & Yi, C.-W. Poly (acrylamide-co-acrylic acid) gel electrolytes for Ni-Zn secondary batteries. *Bull. Korean Chem. Soc.* **34**, 717–718 (2013).
117. Lin, C. et al. Solid-state rechargeable zinc-air battery with long shelf life based on nanoengineered polymer electrolyte. *ChemSusChem* **11**, 3215–3224 (2018).
118. Hwang, H. J. et al. Selective ion transporting polymerized ionic liquid membrane separator for enhancing cycle stability and durability in secondary zinc-air battery systems. *ACS Appl. Mater. Interfaces* **8**, 26298–26308 (2016).
119. Wei, Y. et al. Alkaline exchange polymer membrane electrolyte for high performance of all-solid-state electrochemical devices. *ACS Appl. Mater. Interfaces* **10**, 29593–29598 (2018).
120. Lee, B.-S. et al. Dendrite suppression membranes for rechargeable zinc batteries. *ACS Appl. Mater. Interfaces* **10**, 38928–38935 (2018).
121. Banik, S. J. & Akolkar, R. Suppressing dendrite growth during zinc electrodeposition by PEG-200 additive. *J. Electrochem. Soc.* **160**, D519–D523 (2013).
122. Lan, C. J., Lee, C. Y. & Chin, T. S. Tetra-alkyl ammonium hydroxides as inhibitors of Zn dendrite in Zn-based secondary batteries. *Electrochim. Acta* **52**, 5407–5416 (2007).
123. Nakata, A., Arai, H., Yamane, T., Hirai, T. & Ogumi, Z. Preserving zinc electrode morphology in aqueous alkaline electrolytes mixed with highly concentrated organic solvent. *J. Electrochem. Soc.* **163**, A50–A56 (2016).
124. Hou, Z. G. et al. Surfactant widens the electrochemical window of an aqueous electrolyte for better rechargeable aqueous sodium/zinc battery. *J. Mater. Chem. A* **5**, 730–738 (2017).
125. Lee, C. W., Sathiyanarayanan, K., Eom, S. W., Kim, H. S. & Yun, M. S. Novel electrochemical behavior of zinc anodes in zinc/air batteries in the presence of additives. *J. Power Sources* **159**, 1474–1477 (2006).
126. Mansfeld, F. & Gilman, S. The effect of lead ions on dissolution and deposition characteristics of a zinc single crystal in 6 N KOH. *J. Electrochem. Soc.* **117**, 588–592 (1970).
127. Wang, J. M., Zhang, L., Zhang, C. & Zhang, J. Q. Effects of bismuth ion and tetrabutylammonium bromide on the dendritic growth of zinc in alkaline zincate solutions. *J. Power Sources* **102**, 139–143 (2001).
128. Chu, M. G., Mcbreen, J. & Adzic, G. Substrate effects on zinc deposition from zincate solutions .1. deposition on Cu, Au, Cd and Zn. *J. Electrochem. Soc.* **128**, 2281–2286 (1981).
129. Wei, X. et al. Impact of anode substrates on electrodeposited zinc over cycling in zinc-anode rechargeable alkaline batteries. *Electrochim. Acta* **212**, 603–613 (2016).
130. Gallaway, J. W. et al. An in situ synchrotron study of zinc anode planarization by a bismuth additive. *J. Electrochem. Soc.* **161**, A275–A284 (2014).
131. Wu, T. H., Zhang, Y., Althouse, Z. D. & Liu, N. Nanoscale design of zinc anodes for high-energy aqueous rechargeable batteries. *Mater. Today Nano* **6**, 100032 (2019).
132. Zhao, Z. et al. Long-life and deeply rechargeable aqueous Zn anodes enabled by a multifunctional brightener-inspired interphase. *Energ. Environ. Sci.* **12**, 1938–1949 (2019).
133. Jo, Y. N., Kang, S. H., Prasanna, K., Eom, S. W. & Lee, C. W. Shield effect of polyaniline between zinc active material and aqueous electrolyte in zinc-air batteries. *Appl. Surf. Sci.* **422**, 406–412 (2017).
134. Zhang, Z. et al. Further studies of a zinc-air cell employing a Zn-PCH (PVA chemical hydrogel) anode. *J. Solid State Electrochem.* **22**, 3775–3783 (2018).
135. Zhou, L., Zhou, D., Gan, W. & Zhang, Z. A ZnO/PVA/PAADDA composite electrode for rechargeable zinc-air battery. *Ionics* **23**, 3469–3477 (2017).
136. Gan, W., Zhou, D., Zhou, L., Zhang, Z. & Zhao, J. Zinc electrode with anion conducting polyvinyl alcohol/poly (diallyldimethylammonium chloride) film coated ZnO for secondary zinc air batteries. *Electrochim. Acta* **182**, 430–436 (2015).
137. Zhang, Z., Zhou, D., Li, Z., Zhou, L. & Huang, B. Preparation and properties of a ZnO/PVA/β-CD composite electrode for rechargeable zinc anodes. *ChemistrySelect* **3**, 10677–10683 (2018).
138. Stock, D. et al. Homogeneous coating with an anion-exchange ionomer improves the cycling stability of secondary batteries with zinc anodes. *ACS Appl. Mater. Interfaces* **10**, 8640–8648 (2018).
139. Lee, S.-M. et al. Improvement in self-discharge of Zn anode by applying surface modification for Zn-air batteries with high energy density. *J. Power Sources* **227**, 177–184 (2013).
140. Schmid, M. & Willert-Porada, M. Zinc particles coated with bismuth oxide based glasses as anode material for zinc air batteries with improved electrical rechargeability. *Electrochim. Acta* **260**, 246–253 (2018).
141. Kang, L. et al. Nanoporous $CaCO_3$ coatings enabled uniform zn stripping/plating for long-life zinc rechargeable aqueous batteries. *Adv. Energy Mater.* **8**, 1801090 (2018).
142. Zhao, K. et al. Ultrathin surface coating enables stabilized zinc metal anode. *Adv. Mater. Interfaces* **5**, 1800848 (2018).

143. Schmid, M. & Willert-Porada, M. Electrochemical behavior of zinc particles with silica based coatings as anode material for zinc air batteries with improved discharge capacity. *J. Power Sources* **351**, 115–122 (2017).
144. Pan, J. et al. Advanced architectures and relatives of air electrodes in Zn-air batteries. *Adv. Sci.* **5**, 1700691 (2018).
145. R. Mainar, A. et al. Alkaline aqueous electrolytes for secondary zinc-air batteries: an overview. *Int. J. Energy Res*. **40**, 1032–1049 (2016).
146. Chamoun, M. et al. Hyper-dendritic nanoporous zinc foam anodes. *NPG Asia Mater.* **7**, e178 (2015).
147. Parker, J. F. et al. Rechargeable nickel-3D zinc batteries: an energy-dense, safer alternative to lithium-ion. *Science* **356**, 414–417 (2017).
148. Chao, D. L. et al. A high-rate and stable quasi-solid-state zinc-ion battery with novel 2D layered zinc orthovanadate array. *Adv. Mater.* **30**, 1803181 (2018).
149. Kim, H. et al. Metallic anodes for next generation secondary batteries. *Chem. Soc. Rev.* **42**, 9011–9034 (2013).
150. Kang, Z. et al. 3D Porous copper skeleton supported zinc anode toward high capacity and long cycle life zinc ion batteries. *ACS Sustain. Chem. Eng.* **7**, 3364–3371 (2019).
151. Li, H. F. et al. Enhancement on cycle performance of Zn anodes by activated carbon modification for neutral rechargeable zinc ion batteries. *J. Electrochem. Soc.* **162**, A1439–A1444 (2015).
152. Wang, X. W. et al. An aqueous rechargeable Zn//Co_3O_4 battery with high energy density and good cycling behavior. *Adv. Mater.* **28**, 4904–4911 (2016).
153. Ma, L. T. et al. Initiating a mild aqueous electrolyte Co_3O_4/Zn battery with 2.2 V-high voltage and 5000-cycle lifespan by a Co(III) rich-electrode. *Energy Environ. Sci.* **11**, 2521–2530 (2018).
154. Wilcox, G. D. & Mitchell, P. J. Electrolyte additives for zinc-anoded secondary cells .1. brighteners, levelers and complexants. *J. Power Sources* **28**, 345–359 (1989).
155. Kan, J. Q., Xue, H. G. & Mu, S. L. Effect of inhibitors on Zn-dendrite formation for zinc-polyaniline secondary battery. *J. Power Sources* **74**, 113–116 (1998).
156. Banik, S. J. & Akolkar, R. Suppressing dendritic growth during alkaline zinc electrodeposition using polyethylenimine additive. *Electrochim. Acta* **179**, 475–481 (2015).
157. Mitha, A., Yazdi, A. Z., Ahmed, M. & Chen, P. Surface adsorption of poly-ethylene glycol to suppress dendrite formation on zinc anodes in rechargeable aqueous batteries. *ChemElectroChem* **5**, 2409–2418 (2018).
158. Gomes, A. & Pereira, M. I. D. Pulsed electrodeposition of Zn in the presence of surfactants. *Electrochim. Acta* **51**, 1342–1350 (2006).
159. Ghavami, R. K., Rafiei, Z. & Tabatabaei, S. M. Effects of cationic CTAB and anionic SDBS surfactants on the performance of Zn-MnO_2 alkaline batteries. *J. Power Sources* **164**, 934–946 (2007).
160. Azhagurajan, M. et al. Effect of vanillin to prevent the dendrite growth of Zn in zinc-based secondary batteries. *J. Electrochem. Soc.* **164**, A2407–A2417 (2017).
161. Yang, X. et al. Effective inhibition of zinc dendrites during electro-deposition using thiourea derivatives as additives. *J. Mater. Sci.* **54**, 3536–3546 (2019).
162. Wen, Y. H., Cheng, J., Zhang, L., Yan, X. & Yang, Y. S. The inhibition of the spongy electrocrystallization of zinc from doped flowing alkaline zincate solutions. *J. Power Sources* **193**, 890–894 (2009).
163. Otani, T., Fukunaka, Y. & Homma, T. Effect of lead and tin additives on surface morphology evolution of electrodeposited zinc. *Electrochim. Acta* **242**, 364–372 (2017).
164. Xu, J. J., Ye, H. & Huang, J. Novel zinc ion conducting polymer gel electrolytes based on ionic liquids. *Electrochem. Commun.* **7**, 1309–1317 (2005).